U. S. DEPARTMENT OF THE INTERIOR

U. S. GEOLOGICAL SURVEY

FIELD GUIDE FOR A TRANSECT OF THE CENTRAL SIERRA NEVADA, CALIFORNIA: GEOCHRONOLOGY AND ISOTOPE GEOLOGY

by
R. W. Kistler[1] and R. J. Fleck[1]

Open-File Report 94-267

[1]MS 937, 345 Middlefield Road, Menlo Park, CA 94025

TABLE OF CONTENTS

LIST OF FIGURES

Figure 10.Strontium evolution diagram for whole-rock specimens of Bass Lake Tonalite collected along Hwy. 41 to the north of the Coarse Gold roof pendant. Variation in magnetic susceptibility iscorrelated with the variation in initial $^{87}Sr/^{86}Sr$ values of the rocks. Rocks with high susceptibility (magnetite bearing) or low susceptibility (ilmenite bearing) had initial $^{87}Sr/^{86}Sr$ values greater than or less than 0.7060, respectively. Specimen BL1 is a quartzite at the contact between the intruded metamorphosed sedimentary rocks and the pluton.

Figure 11. Generalized geology of the intrusive suite of Yosemite Valley (modified from Bateman, 1992). The location for field trip stops 9 and 10 are shown by numbered dots.

Figure 12. Map of the Tuolumne Intrusive Suite (modified from Kistler and others, 1986). Sample Traverses: AB and CD (Bateman and Chappell, 1979) and EC (Kistler, 1974). Asterisks are specimen locations in the Hetch Hetchy quadrangle (Kistler, 1974). All whole-rock isotopic data from specimens along these traverses is summarized in Table 2 (modified from Kistler and others, 1986). Locations of field trip stops 7, 8, 12, 13, 14, 15, and 16 are shown by numbered dots.

Figure 13.Rb-Sr whole-rock isochron plot for specimens of intrusive suite of Yosemite Valley (El Capitan, Taft, Arch Rock, Hoffman, and Ten Lakes plutons). The specimen of Taft Granite is not included in the isochron regression.

Figure 14. Multiple technique and mineral age-profile along traverse AB of Figure 12 except the westernmost data are from sample FD13 at Washburn Point (field trip stop 7). The x--x--x line for $^{40}Ar/^{39}Ar$ on K-feldsparspar plot s the minimum and maximum ages determined during argon release that did not yield a plateau. The central (x) is the calculated total gas age for these minerals.

Figure 15. Triangular diagram showing K_2O, Na_2O, and CaO in rocks of the Tuolumne Intrusive Suite (modified from Kistler and others, 1986). Chemically coherent fields are indicated for different rock types showing the range of initial $^{87}Sr/^{86}Sr$: asterisks (0.7057-0.7061), tonalite of Glacier Point, tonalite of Glen Aulin and granodiorite of Kuna Crest; solid triangles (0.7057-0.7063), inner and outer parts of the Half Dome Granodiorite; solid squares (0.7064-0.7065), outer part of the Cathedral Peak Granodiorite; open squares (0.7063-0.7064), inner part of the Cathedral Peak Granodiorite; solid circles (>0.7066), Johnson Granite Porphyry;.open circles (0.7064-0.7067), Sentinel Granodiorite and granodiorite of Yosemite Creek.

Figure 16. Geologic map of the Long Valley region showing the distribution of volcanic rocks related to Long Valley caldera magmatic system and the younger Inyo-Mono magmatic system (modified from Hill and others, 1985). Field trip stops 18, 19, and 20 are shown by numbered dots.

Figure 17. Geologic map of the Mono Craters and domes (modified from Wood, 1983). Field trip stop 20 is Panum Dome, the northernmost volcano in the chain.

Figure 18.Rb-Sr whole-rock isochron plot for specimens of host granite, mafic inclusions, and a synplutonic dike of the granite of Lee Vining Canyon. Sources of data are given in the text.

Figure 19. Plot of $\varepsilon_{Nd}(0)$ vs magnetic susceptibility in SI units for specimens of granite of Lee Vining Canyon host rocks, mafic inclusions, and a synplutonic dike.

Figure 20. Rb-Sr whole-rock isochron diagram for volcanic rocks and associated plutons of the lower Koip sequence.

LIST OF TABLES

Introduction

The Sierra Nevada batholith is composite and is made up of plutons that range in composition from gabbro to granite and in age from Triassic (ca. 240 Ma) to Late Cretaceous (ca. 77 Ma). The plutons intrude wall rocks of metamorphosed sedimentary rocks of Late Proterozoic to Permian age and sedimentary and volcanic rocks of Triassic to Early Cretaceous age. This field trip will emphasize the plutonic rocks, and stops will be in plutons that represent most of the spectrum of compositions and ages that occur in the batholith.

The age distribution of plutons in the Sierra Nevada batholith is shown in Figure 1. Plutons occur in long, linear belts, with those of different age defining distinct trends. The more northerly-trending Cretaceous belts cut across the older more northwesterly trending belts of Triassic and Jurassic age. Initial $^{87}Sr/^{86}Sr$ in plutons of the Sierra Nevada varies with geographic position from about 0.703 to 0.708. In California and Nevada, the initial $^{87}Sr/^{86}Sr = 0.706$ isopleth coincides nicely with wall-rock sedimentary-facies boundaries (Figure 2) and correlates with variations in chemical characteristics of the plutons. This isopleth is interpreted to represent the approximate position of the cryptic western margin of Precambrian sialic basement in the Sierra Nevada (Kistler and Peterman, 1973).

Kistler (1990, 1993) related differences in the regional pattern of $\delta^{18}O$ in Sierra Nevada plutons to their derivation from and emplacement into two different lithosphere types, now in tectonic contact. Differences between these lithospheric sources are also reflected in the major-element (Ague and Brimhall, 1988), minor-element (e.g., Rb, Kistler, 1990), and lead-isotopic (Chen and Tilton, 1991) compositions of the plutons. Lithosphere east of the tectonic boundary has the chemical and isotopic characteristics of, and is continuous with, the North American continent. Plutons west of the boundary reflect differences assigned by Kistler (1990, 1993) to the Panthalassan terrane.

On the first day our trip will start in Fresno and progress eastward to examine Early Cretaceous plutons just south of 37°N. Latitude (Figure 1). We will continue eastward through the extensive dioritic to tonalitic plutons of the western Sierra Nevada to visit the contact zone between Early Cretaceous and Late Cretaceous granodiorite plutons just to the south of the Dinkey Creek roof pendant. A shear zone in the Early Cretaceous plutons at this site is thought to be an exposed remnant of the tectonic boundary between the two lithosphere types that has not been engulfed by Late Cretaceous plutons (Kistler, 1993). On the second day, we will start again from Fresno and travel north across Early Cretaceous tonalite-trondhjemite plutons of the western Sierra Nevada, making several stops. Within this part of the traverse, we again cross the major lithospheric boundary, but its location can only be determined by the change in the chemical and magnetic character of the tonalites. Entering Yosemite National Park by the south entrance, we will examine the complex intrusive zone between Early Cretaceous plutons and the Late Cretaceous Tuolumne Intrusive Suite in the area south of Yosemite Valley. The Tuolumne Suite is one of five Late Cretaceous zoned plutons or plutonic complexes exposed in the highest elevations of the eastern Sierra Nevada (Figure 3). We will spend the night in Yosemite Valley. The Visitors Center and Museum have impressive displays of the geology, biology, and history of Yosemite, which participants may wish to examine on their own during the evening. On the third day, we will leave Yosemite Valley and travel north and east to visit exposures of the rocks of the Tuolumne Intrusive Suite and cross the high Sierra. We will spend the night at Mammoth Lakes in the eastern Sierra Nevada. On the fourth day, we will take advantage of our location near Long Valley to examine exposures of the Pleistocene Bishop tuff, one of the first recognized ignimbrites. We will also visit a Holocene rhyolite dome in the Mono Craters chain; a broad, mafic-enclave zone in a Triassic granite near its contact with metamorphosed Paleozoic sedimentary rocks; and, finally, a small alkalic pluton that is the remnant of a Triassic volcanic neck near Saddlebag Lake. The day will start and end in Mammoth Lakes. On the fifth day, we will leave Mammoth Lakes and retrace our path across Tioga Pass and Yosemite National Park, leaving by the north entrance on California Highway 120. We expect to arrive back in Berkeley in mid-afternoon.

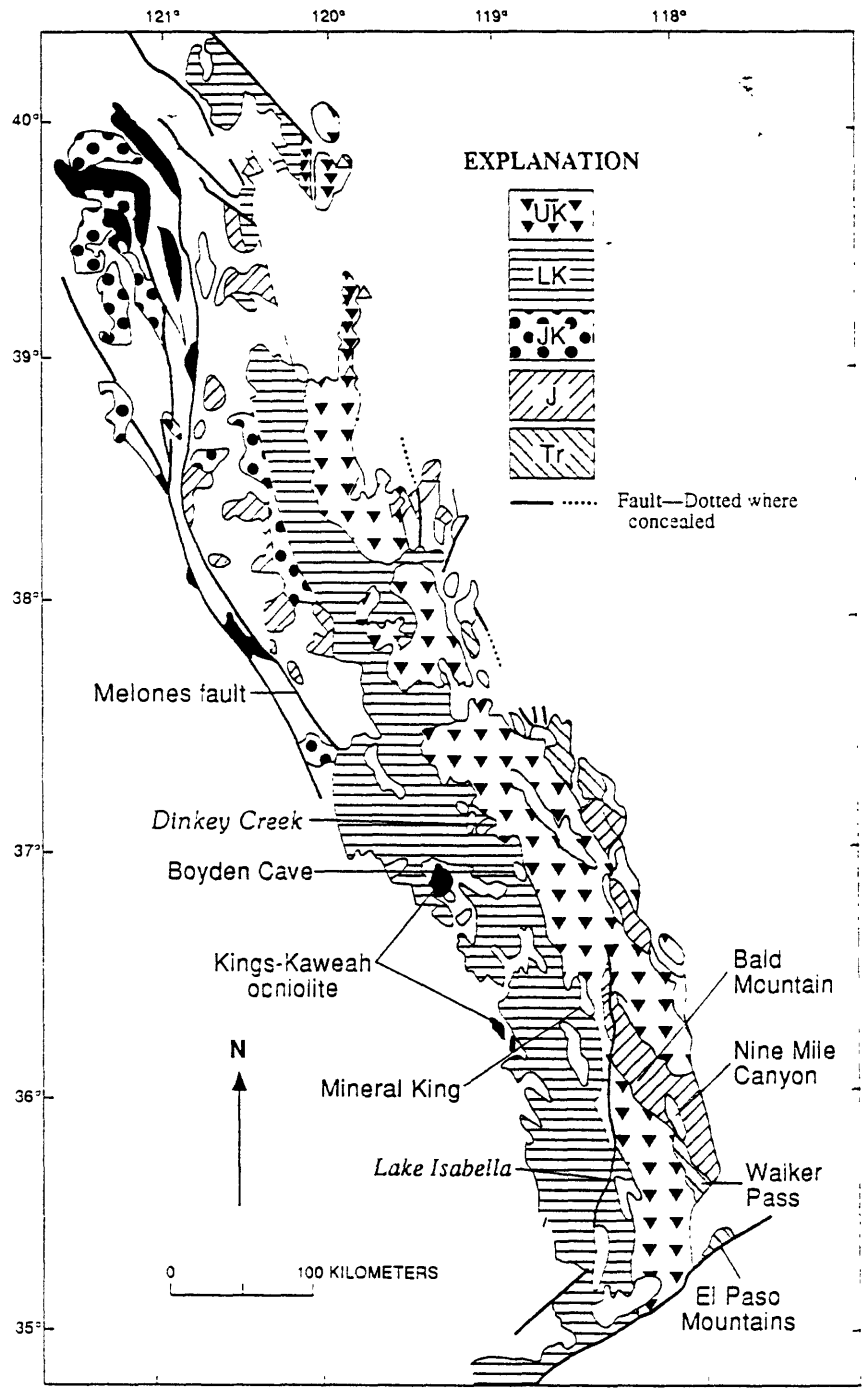

Figure 1. Map of the Sierra Nevada showing the age distribution of plutonic rocks. The solid black pattern is for ophiolites in the western Sierra Nevada. Pluton ages: UK, Late Cretaceous (92-77 Ma); LK, Early Cretaceous (123-100 Ma); JK, Late Jurassic and Early Cretaceous (152-127 Ma); J, Middle Jurassic (180-165 Ma); Triassic (240-200 Ma).

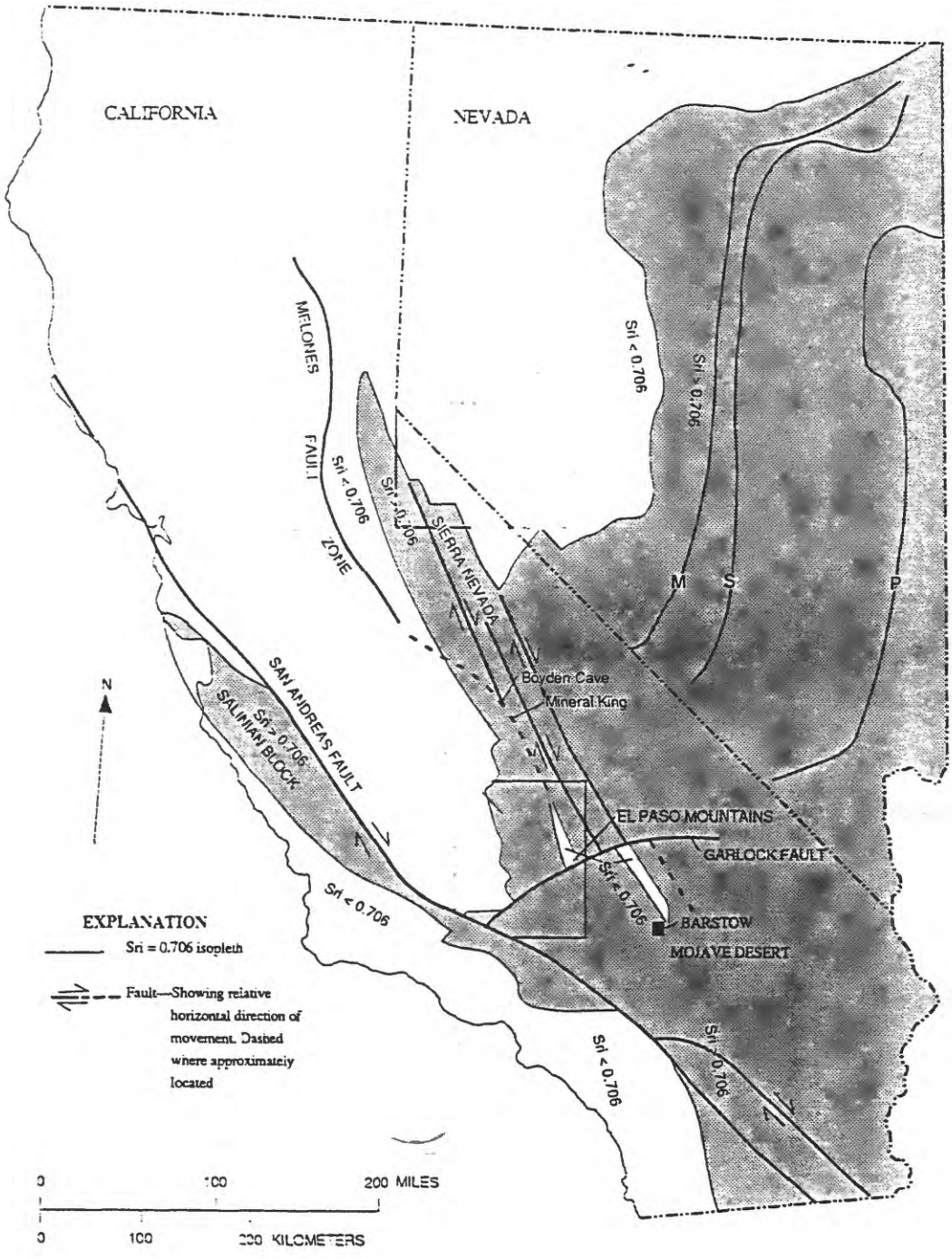

Figure 2. Outline map of California and Nevada showing the initial $^{87}Sr/^{86}Sr$=0.706 isopleth for plutonic rocks in the region. Facies boundaries: belt of Permian rugose corals (P); Silurian shelf-slope break (S); belt of thickest Lower Mississippian foreland clastic deposits (M). Figure is modified from Kistler (1990).

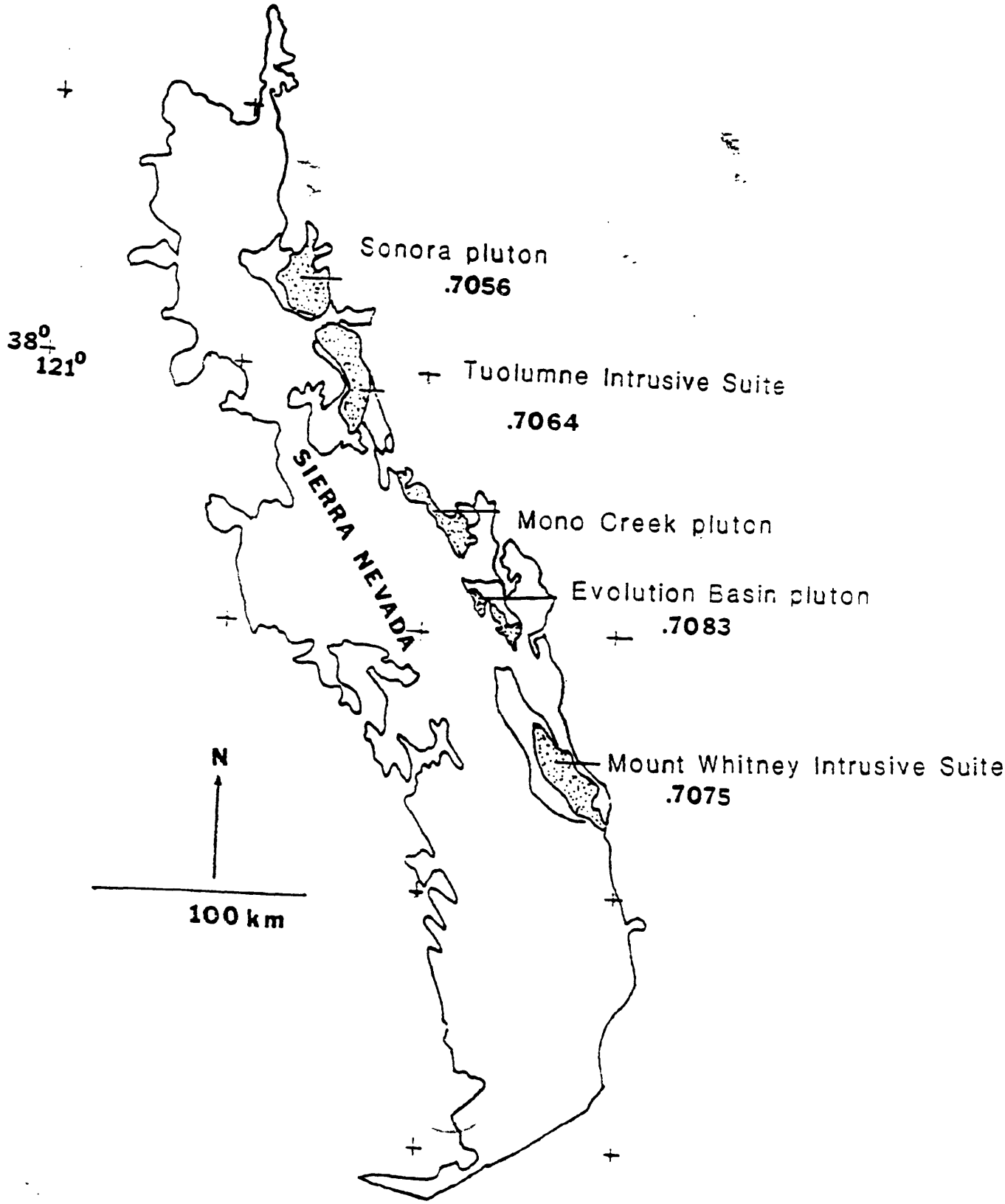

Figure 3. Outline map of granitoid exposures in the composite Sierra Nevada batholith. The Tuolumne Intrusive Suite is one of five compositionally zoned plutons of Late Cretaceous age (93 to 77 Ma) that crop out along the crest of the Sierra Nevada. The youngest porphyritic facies of each suite is shown in a stippled pattern. The initial $^{87}Sr/^{86}Sr$ values for these porphyritic rocks are indicated on the diagram.

ROAD LOG

DAY 1. Fresno to Courtright Reservoir and Return

Mileage: Cumulative distance is shown in miles. (Interval mileage from the preceding stop is shown in parentheses.)

0.0 (0.0) Begin road log at the intersection of California Highways 41 and 168 in Fresno, California. Travel north on Hwy 41 (Eisenhower Freeway) to Herndon Avenue Exit (East) a distance of about 1.8 miles. Turn east on Herndon Avenue, traveling for about 6.2 miles to Hwy 168 (Tollhouse Road). Turn left and proceed northeast on Hwy 168 to the entrance road to Academy quarry, on the south side of Hwy 168 about 1 mile past the small village of Academy. We will park near the quarry offices on the main level.

18.7 (18.7) Stop #1. Academy pluton, Academy quarry.

The Academy pluton (Figure 4) is concentrically zoned and ranges in composition from olivine-hornblende melagabbro to hornblende-biotite granodiorite, and is believed to represent the roots of a Cretaceous calc-alkaline volcano (Mack and others, 1979). The quarry stop is in the quartz norite unit. Data:

K-Ar: hornblende 124 Ma, biotite 115 Ma (Kistler, Bateman, Brannock, 1965), plagioclase 108 Ma, augite 99 Ma, hypersthene 50 Ma (Kistler and Dodge, 1966).
U-Pb zircon: quartz norite, 120 Ma, pyroxene quartz diorite 121 Ma, Biotite-hornblende quartz diorite, 114 Ma (Saleeby and Sharp, 1980).
$\delta^{18}O$ = +7.0 per mil, $^{143}Nd/^{144}Nd = 0.51288$, $\varepsilon_{Nd}T$ = +4.2, $(^{87}Sr/^{86}Sr)_o = 0.70382$ (Kistler, 1993, Figure 5, Table 1, #25) for the whole-rock specimen, CL-1, that was used for the K-Ar mineral ages.

The pyroxenes were dated by the K-Ar technique to investigate the possibility of excess argon in them. Rather than having too much ^{40}Ar, they were deficient in argon content. An event to cause the deficiency and the young apparent age of the hypersthene is not known. Kistler and Dodge (1966) suggested that exsolution lamellae observed in the mineral produced a diffusion dimension much smaller than the actual crystal size and permitted partial loss of accumulated radiogenic argon at very low temperature.
The Academy pluton intrudes the northern end of the Kings-Kaweah ophiolite (Figure 1), a 125-km-long, northwest-trending zone of highly deformed mafic and ultramafic rocks. Sm-Nd whole-rock and mineral data for the Kings River ophiolite define two ages of ophiolite formation at 485±21 Ma and 285±45 Ma with ε_{Nd} (485 Ma) = +10.7±0.5 and ε_{Nd} (285 Ma) = +9.9±1.1, respectively (Shaw and others, 1987).

Leave the quarry and continue north on Hwy 168 for 15.6 miles to the junction with Lodge Road. Turn left at the stop sign to stay on Hwy 168. Park off the highway.

34.3 (15.6) Stop #2. Bass Lake Tonalite

We examine a roadcut exposure on the north side of Hwy 168 at the Lodge Road turnoff to the town of Tollhouse. The rock exposed is Bass Lake Tonalite, the extensive member of the Early Cretaceous Fine Gold Intrusive Suite (Figure 6). This major granitoid rock unit of the west-central Sierra Nevada is predominantly equigranular, typically medium-gray, medium-grained, hornblende-biotite tonalite to granodiorite, but includes minor quartz diorite and granite facies. A layered mafic dike intrudes the tonalite at this exposure, and magnetic susceptibility of both rock types ranges from 2 to 4 units on the Kappa meter. In

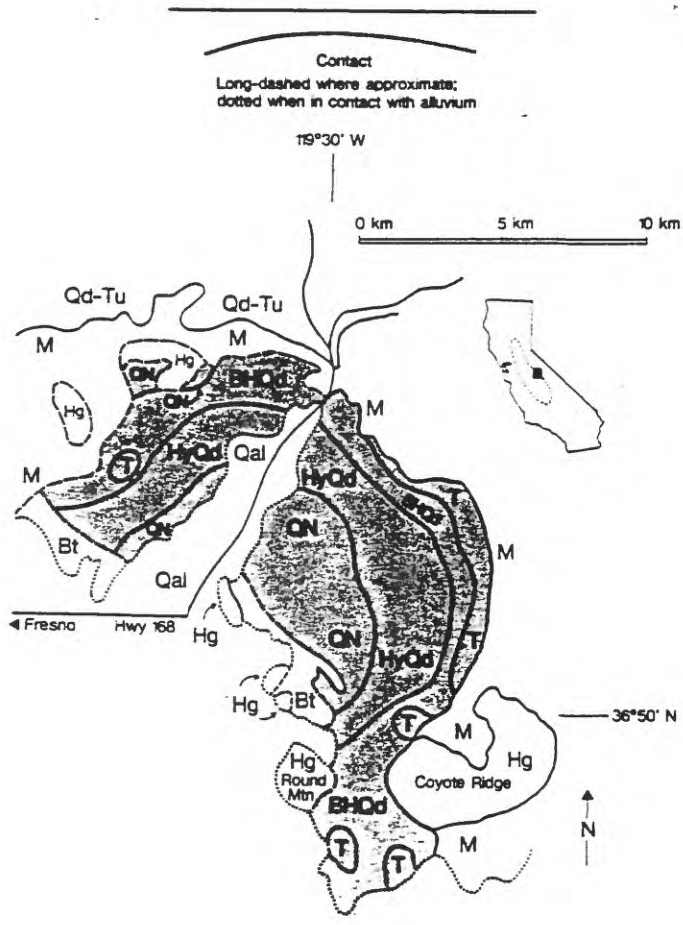

Figure 4. Map showing distribution of rock units in the Academy pluton (modified from Mack and others, 1979). Map units: Qal, unconsolidated Quaternary deposits; Qd-Tu, undifferentiated quartz diorite and tonalite; Bt, biotite tonalite; T, tonalite; BHQd, biotite-hornblende quartz diorite; HyQd, hypersthene quartz diorite; QN, quartz norite; Hg, hornblende gabbro; M, Pre-Cretaceous, undifferentiated metamorphic rocks. The Academy pluton is shaded gray.

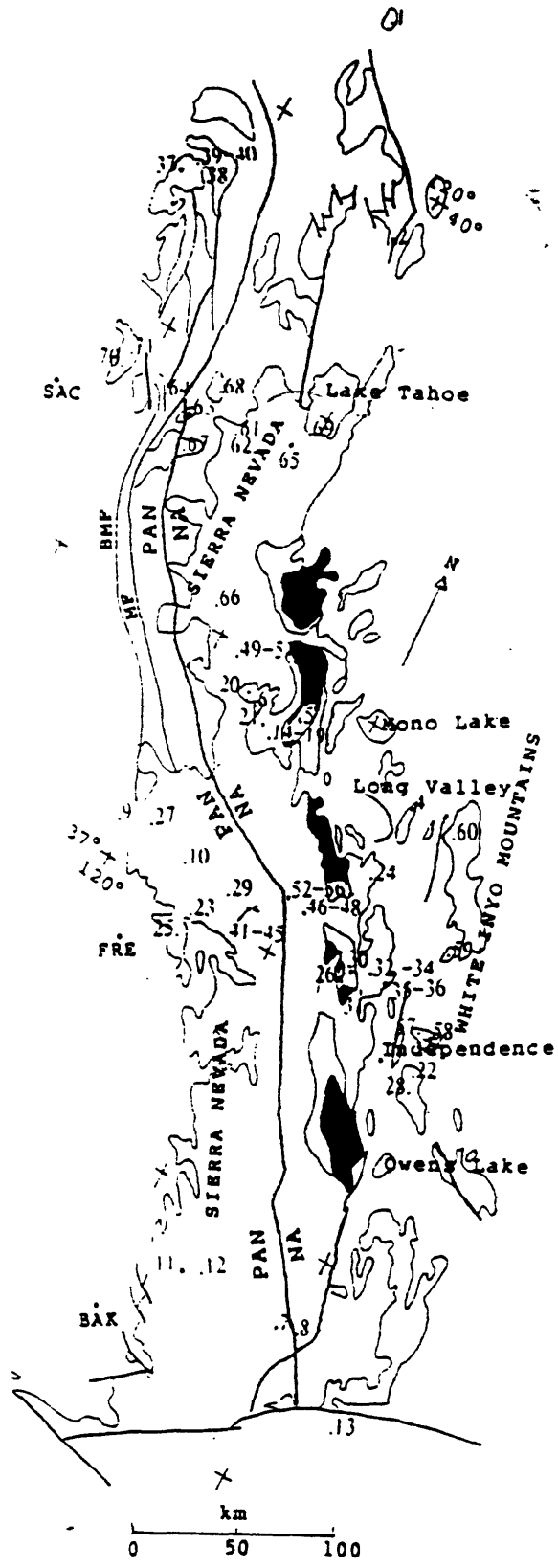

Figure 5. Map showing the outline of exposures of Mesozoic granitoid rocks in the Sierra Nevada and Inyo-White Mountains, California. The porphyritic central facies of the five zoned intrusive suites of the Late Cretaceous (92-77 Ma) Cathedral Range intrusive epoch that crop out along the crest of the Sierra Nevada (Evernden and Kistler, 1970; Kistler and others, 1986) are shown in black. Locations of granitoid rock specimens that have measured initial Sr and Nd isotopic values (Table 1) are shown by numbered dots. The tectonic boundary between North American lithosphere (NA) to the east and Panthalassan lithosphere (PAN) to the west is shown as a heavy solid line

spite of the mafic, iron-rich character of the Fine Gold Intrusive Suite, the magnetic susceptibility is the lowest of granitoid rocks exposed in the Mariposa 1°x2° quadrangle (Figure 7) and the opaque oxide in the rocks is ilmenite (Bateman and others, 1991). Correlations of magnetic susceptibility with initial $^{87}Sr/^{86}Sr$ in a study area of the Fine Gold Intrusive Suite suggest that oxidation ratios have been inherited from the source regions for the magmas from which the rocks crystallized. Magnetic susceptibility may also be affected by reduction of Fe^{3+} to Fe^{2+} by organic carbon or other reducing substances scavenged from intruded metasedimentary wall rocks. On the last day of this trip, we will look at some rocks that probably illustrate this phenomenon.
Data:

K-Ar (From several different locations in the Fine Gold Intrusive Suite): hornblendes, 118-114 Ma; biotites, 114-91 Ma. Late Cretaceous apparent ages of biotite are the result of resetting by younger, 90-Ma plutons (Kistler , Bateman, and Brannock, 1965).
U-Pb zircons: 124 Ma to 105 Ma (Stern, Bateman, Morgan, Newell, and Peck, 1981). Map Nos. 9, 10, 23, 25, and 27 (Figure 5, Table 1) represent localities of specimens from the Fine Gold Intrusive Suite that have Nd, Sr, and oxygen isotopic data.

Continue east on Hwy 168 from Stop #2 for another 14.4 miles to Dinkey Creek Road, just south of the town of Shaver Lake. Take Dinkey Creek Road east 11.8 miles to U.S. Forest Service Road 40 just south of Dinkey Creek. Turn southeast on USFS Road 40 to McKinley Grove (about 5.8 mi.).

66.3 (32.0) Stop #3. McKinley Grove of *Sequoia gigantea* trees.

The rock is biotite granite of McKinley Grove, an Early Cretaceous pluton of the Shaver Intrusive Suite (104-100 Ma; Figure 8). Map #29 and 41-45 (Figure 5, Table 1) are specimens from the Shaver Intrusive Suite that have Nd, Sr, and oxygen data.

Leave McKinley Grove and continue southeast on USFS Road 40 for 8.1 miles to the Courtright Road turnoff. Turn left (north) from USFS Road 40 on Courtright Road and continue about 7.8 miles to the parking area by Courtright Reservoir.

82.2 (15.9) Stop #4 Courtright Geologic area (Bateman, Kistler, and DeGraff, 1984).

We walk from the Courtright parking area toward the dam, using the published field guide to geologic features exposed at the Courtright Intrusive Zone (Bateman, Kistler, and DeGraff, 1984). We will view intrusive contacts between the Mount Givens Granodiorite of the John Muir Intrusive Suite and two plutons of the Shaver Intrusive Suite, the Dinkey Creek Granodiorite and the granite of Lost Peak. A shear zone in the plutons of the Shaver Intrusive Suite coincides with the boundary between Panthalassan and North American lithospheres (Figure 5, Kistler, 1990, 1993).
Data:

Mt. Givens Granodiorite:
K-Ar: hornblende, 89.2 and 89.2 Ma; biotite, 88.2 and 87.2 Ma (Kistler, Bateman, and Brannock, 1965).
Fission Track: apatite, 91 and 84 Ma; sphene, 83 and 87 Ma (Naeser and Dodge, 1969).
$^{40}Ar/^{39}Ar$: hornblende, 90.2 and 89.2 Ma; biotite, 87.7 and 87.2 Ma (Tobisch, Renne, and Saleeby, 1993).

Table 1. Nd, Sr, and oxygen isotopic data for Sierra Nevada plutons and wall-rocks

Plutonic Rocks

Map No.	Sample No.	$\varepsilon_{Nd}T$	$(^{87}Sr/^{86}Sr)_o$	$\delta^{18}O$	Age (Ma)	Rock unit
1.	73-2	+5.1[a]	0.7037[f]	+7.5[k]	121	Eagle Lake pluton
2.	73-3	+1.2[a]	0.7048[f]	+8.2[k]	88	Beckwourth Pass pluton
3.	73-5	+2.5[a]	0.7043[f]		90	Lake Tahoe pluton
4.	73-9	-3.5[a]	0.7052[f]	+8.2[k]	210	Wheeler Crest Granodiorite
5.	73-14	-6.3[a]	0.7065[f]	+8.2[k]	87	Cathedral Peak Granodiorite
6.	73-15	-3.9[a]	0.7065[f]	+8.3[k]	107	El Capitan Granodiorite
7.	73-25	-7.6[a]	0.7082[f]	+11.0[k]	79	Granodiorite of Claraville
8.	73-26	+2.2[a]	0.7036[f]	+7.8[k]	240	Granodiorite of Walker Pass
9.	73-28	+6.5[a]	0.7032[f]	+9.2[k]	126	Trond. of Sherman Thomas
10.	73-29	+3.3[a]	0.7044[f]		103	Bass Lake tonalite
11.	78-3	+6.0[a]	0.7032[g]	+7.3[k]	120	Ton. Carver Bowen Ranch
12.	78-4	-2.4[a]	0.7066[g]	+9.4[k]	90	Granodiorite of Alder Creek
13.	78-17	-6.3[a]	0.7066[g]	+10.2[k]	74.2	Granodiorite of Randsburg
14.	K46-64	-3.2[b]	0.7057[b]		90	Tonalite of Glacier Point
15.	Z-53	-3.9[b]	0.7059[b]	+7.7[b]	88	Tonalite of Glen Aulin
16.	Z-58	-5.3[b]	0.7063[b]	+8.3[b]	86	inner Half Dome Grano.
17.	Z-63	-5.2[b]	0.7065[b]		86	outer Cathedral Peak Grano.
18.	SSr-T1	-6.3[b]	0.7065[b]		84	inner Cathedral Peak Grano.
19.	Z-18	-8.0[b]	0.7066[b]	+8.3[b]	81	Johnson Granite Porphyry
20.	K5-64	-4.5[b]	0.7065[b]		92	Sentinel Granodiorite
21.	K37-67	-5.9[b]	0.7067[b]		92	Sentinel Granodiorite
22.	FD-2	-3.2[c]	0.7059[c]	+9.1[c]	170	Hunter Mountain Qtz. Mon.
23.	WV-1	+3.2[c]	0.7043[c]	+9.2[c]	118	Tonalite south of Black Mtn.
24.	MT-1	-5.9[c]	0.7061[c]	+9.3[c]	210	Wheeler Crest Granodiorite
25.	CL-1	+4.2[c]	0.7038[c]	+7.0[c]	125	Academy pluton
26.	R-99	-2.2[c]	0.7093[c]	+7.4[c]	86	Evolution Basin pluton
27.	FD-20	-0.4[c]	0.7042[c]	+10.6[c]	112	Granodiorite of Knowles
28.	FD-3	-7.7[c]	0.7069[c]	+8.6[c]	170	Paiute Monument Qtz. Mon.
29.	JB-1	-3.4[c]	0.7065[c]	+9.9[c]	118	Bass Lake Tonalite
30.	MG-1	-3.0[c]	0.7066[c]	+7.8[c]	88	Lamarck Granodiorite
31.	PAL 3	-3.3[c]	0.7062[c]	+7.0[c]	107	Inconsolable Granodiorite
32.	PAL 61	-6.7[c]	0.7072[h]	+7.3[c]	169	Tinemaha Granodiorite
33.	PAL 8	-7.2[c]	0.7072[h]	+8.5[c]	169	Tinemaha Granodiorite
34.	PAL 53xe	-6.9[c]	0.7072[h]	+7.7[c]	169	mafic incl. in Tine. Grano.
35.	PAL 30	-5.0[c]	0.7065[h]	+7.3[c]	171	Grano. of McMurray Mead.
36.	PAL 72	-5.0[c]	0.7065[h]	+9.2[c]	171	Grano. of McMurray Mead.
37.	BR 1	+7.2[c]	0.7036[c]	+7.4[c]	133	Bald Rock Tonalite
38.	BR 8	+7.7[c]	0.7036[c]	+7.1[c]	133	Bald Rock Trondjhemite (a)
39.	BR 13	+7.3[c]	0.7036[c]	+6.4[c]	133	Bald Rock Trondjhemite (a)
40.	BR 3	+5.9[c]	0.7038[c]	+10.2[c]	133	Bald Rock Trondjhemite (b)
41.	SLB-93X3	-7.7[d]	0.7075[d]		104	Dinkey Creek Granodiorite
42.	Kdc20a	-7.3[e]	0.7075[e]		104	Dinkey Creek Granodiorite
43.	Kdc22i	-6.6[e]	0.7075[e]		104	mafic inclusion (Din. Cr.)
44.	Kdc26i	-5.2[e]	0.7075[e]		104	mafic inclusion (Din. Cr.)
45.	Kdc02m	-6.3[e]	0.7068[e]	+7.9[c]	104	schlieren (Dinkey Creek)
46.	Kmg41a	-3.8[e]	0.7065[e]		88	Mount Givens Granodiorite
47.	Kmg48m	-2.6[e]	0.7065[e]		88	schlieren (Mt. Givens Grano)

Table 1 (continued)

Map No.	Sample No.	$\varepsilon_{Nd}T$	$(^{87}Sr/^{86}Sr)_o$	$\delta^{18}O$	Age (Ma)	Rock unit
48.	Kmg45i	-2.3[e]	0.7057[e]		88	mafic inclusion (Mt. Givens)
49.	Kpv-1	-4.4[e]	0.7060[e]		114	grano. of Poopenaut Valley
50.	Ipv	-4.0[e]	0.7060[e]		114	mafic inclusion (Gran. Poop)
51.	Epv1	-0.7[e]	0.7050[e]		114	dike (Grano. Poopenaut Val.)
52.	EAGPK54	-7.1[j]	0.7079[j]		91	Eagle Peak pluton
53.	EAGPK91	-5.9[j]	0.7075[j]	+9.9[j]	91	Eagle Peak pluton
54.	EAGPK97	-7.6[j]	0.7081[j]		91	Eagle Peak pluton
55.	EAGPK-c1	-4.9[j]	0.7075[j]	+9.7[j]	91	Eagle Peak pluton
56.	EAGPK-e83	-5.3[j]	0.7074[j]		91	Eagle Peak pluton
57.	PF98	-18.5[c]	0.7103[i]	+9.8[l]	80	Papoose Flat pluton
58.	PapFla	-6.8[c]	0.7066[f]	+8.4[k]	80	Papoose Flat pluton
59.	BC-C-24	-19.8[c]	0.7121[i]	+9.6[i]	81	Birch Creek pluton
60.	BNPK-1	-12.8[c]	0.7077[i]	+9.0[i]	74	Boundary Peak pluton
61.	SCC-33	-0.8[c]	0.7050[c]	+7.5[c]	141	HWY 50 unnamed
62.	SCD-14	-4.1[c]	0.7060[c]	+8.3[c]	105	HWY 50 unnamed
63.	SCC-29	+4.2[c]	0.7040[c]	+6.9[c]	127	Mosquito Camp pluton
64.	SCC-25	+6.7[c]	0.7032[c]	+7.3[c]	138	Coloma pluton
65.	SCD-11	-3.4[c]	0.7058[c]	+8.4[c]	100	Lovers Leap pluton
66.	SCH-8	-2.7[c]	0.7067[c]	+7.9[c]	141	Long Barn pluton
67.	SCC-5	+1.6[c]	0.7047[c]	+7.3[c]	127	Somerset pluton
68.	Scc-1	-4.1[c]	0.7034[c]	+9.6[c]	170	Pino Grande pluton
69.	SCD-6	+0.1[c]	0.7053[c]	+8.0[c]	91	Echo Lake pluton
70.	AA-5	+2.8[c]	0.7037[c]	+8.5[c]	136	Rocklin pluton
71.	AA-26	+5.6[c]	0.7033[c]	+7.0	148	Penryn pluton
Wall Rocks						
72.	FD-33	+4.6[a]	0.7041[f]		100	Jur. volc. rock comp.
73.	FD-46	-6.6[a]	0.7120[f]		100	Paleo. sed composite
74.	FD-39	-10.8[a]	0.7135[f]		100	Paleo. sed composite
75.	R RPV-1	-2.2[a]	0.7084[f]		100	Ritter Range composit
76.	PC30a	-15.6[a]	0.7360[f]		100	PreCambrian sediments
77.	B-37	-11.5[a]	0.7150[f]	+14.8[a]	100	granulite xenolith
78.	OC-1	+8.3[d]	0.7030[d]		100	spinel lherzolite
77	P-1	+4.8[d]	0.7040[d]		100	gar-hbde lherzolite
77.	F-99	-6.0[d]	0.7065[d]	+7.8[c]	100	grospydite
77.	B-75	+0.8[d]	0.7049[d]	+5.3[c]	100	garnet pyroxenite eclog.
77.	B-3	-7.8[d]	0.7072[d]	+9.2[c]	100	garnet granulite
77.	B-45	-0.9[d]	0.7053[d]	+8.6[c]	100	plag. amphibolite
77.	B-9	-3.5[d]	0.7062[d]	+7.4[c]	100	hornblende hornfels
77.	B-60	-17.4[d]	0.7316[d]	+9.9[c]	100	sillimanite gneiss
79.	PS-9	+0.2[c]	0.7051[c]		104	clinopyroxenite
79.	PS-11	-2.2[c]	0.7081[c]		104	clinopyroxenite
79.	PS-14	-7.8[c]	0.7091[c]		104	garnet websterite

Note: $\varepsilon_{Nd}T=([^{143}Nd/^{144}Nd_{rock}T/^{143}Nd/^{144}Nd_{CHUR}T]-1)*10^4$ where T=age and $^{143}Nd/^{144}Nd_{CHUR}T=0.512642-0.1967(e^{0.00654T}-1)$. $\delta^{18}O$ is the relative difference in isotopic ratio between a sample and SMOW (standard mean ocean water), expressed in parts per thousand. *References*: a. DePaolo, 1981. b. Kistler and others, 1986. c. Kistler, 1993. d. Domenick and others, 1983. e. Barbarin and others, 1989. f. Kistler and Peterman, 1973. g. Kistler and Peterman, 1978. h. Sawka and others, 1990. i. Griffis, 1987. j. Hill and others, 1988. k. Masi and others, 1981.

Rb-Sr whole-rock isochron (Figure 9a): 86.8±2.4 Ma, $(^{87}Sr/^{86}Sr)_o = 0.70652$, $\varepsilon_{Nd}T = -3.8$ (Barbarin, Dodge, Kistler, and Bateman, 1989; Dodge and Kistler, 1990).

Rb-Sr mineral isochron (Figure 9a): 87±2 Ma, $(^{87}Sr/^{86}Sr)_o = 0.70693$ (Hill, O'Neil, Noyes, Frey, and Wones, 1988).

U-Pb zircon: 92.8 and 87.8 Ma (Stern and others, 1981); 90±3 Ma (Tobisch, Renne, and Saleeby, 1993).

Granodiorite of Dinkey Creek:

Rb-Sr whole-rock isochrons: 101 Ma, $(^{87}Sr/^{86}Sr)_o = 0.7071$, (Evernden and Kistler, 1970), 103.2 ± 2.2 Ma, $(^{87}Sr,^{86}Sr)_o = 0.7075, 0.7072$, $\varepsilon_{Nd}T = -7.7$ to -7.0, (Figure 9b, Dodge and Kistler, 1990, Barbarin, Dodge, Kistler, and Bateman, 1989).

U-Pb zircon: 102±1 Ma (Tobisch, Renne, Saleeby, 1993), 104 Ma. (Stern, Bateman, Morgan, Newell, and Peck, 1981).

$^{40}Ar/^{39}Ar$ <1 km from Mt. Givens Granodiorite hornblende, 90.5, 91.5, and 90.2 Ma; biotite, 88.7, 87.5, and 88.7 Ma (Tobisch, Renne, and Saleeby, 1993).

$^{40}Ar/^{39}Ar$ >1 km from Mt. Givens Granodiorite hornblende, 94.0 Ma; biotite, 88.6 Ma (Tobisch, Renne, and Saleeby, 1993).

After completing the Courtright Intrusive Zone field guide, leave the parking area by Courtright Dam and return to Fresno by Courtright Road, USFS Road 40, Dinkey Creek Road, Hwy 168, Herndon Rd, and Hwy 41. The distance is about 82 miles and requires a little over 2 hours.

Day 2. Fresno to Yosemite Valley.

0.0 **(0.0)** Begin road log at the intersection of California Highways 41 and 168 in Fresno, California. Travel north on Hwy 41 (Eisenhower Freeway) toward Yosemite National Park for 22.9 miles to the junction with Road 200 (O'Neals turnoff). Turn south (right) on Road 200 for about 0.2 miles to an unpaved road on the north (left) side. Turn north (left), traveling about 0.2 miles and stop at a roadcut exposure of Ward Mountain Trondhjemite.

23.3 (23.3) Stop #5. Ward Mountain Trondhjemite.

The Ward Mountain Trondhjemite is a phase of the Fine Gold Intrusive Suite (Figure 6) and may represent several indistinguishable plutons. A mafic synplutonic dike is exposed in the leucocratic trondhjemite in the roadcut exposure. The magnetic susceptibility of the trondhjemite and the mafic dike is about 0.1 and 0.3 to 0.5 units, respectively, on the Kappa meter, indicating that both rock facies are in the ilmenite series (Ishihara, 1977) of granitoid rocks. A U-Pb zircon age from a separate but correlative pluton to the north of these exposures is 115 Ma (Stern, Bateman, Morgan, Newell, and Peck, 1981).

Return to Hwy 41, turn north (right), and continue toward Yosemite National Park. For the next 9.5 miles to the north we will be passing through tonalite and trondhjemite exposures of the Early Cretaceous, Fine Gold Intrusive Suite. At the town of Coarsegold we enter a roof pendant of metamorphosed sedimentary and volcanic rocks, including the phyllite of Briceburg (Triassic), the phyllite and chert of Hite Cove (undivided), and the Middle and/or Early Jurassic greenstone of Bullion Mountain (187±10 Ma, Rb-Sr whole-rock isochron) (Bateman, Harris, Kistler and Krauskopf, 1985). We travel across metamorphic rocks for about three miles and then pass into more Bass Lake Tonalite, north of the Coarsegold roof pendant. This tonalite, dated at 108 and 105 Ma by U-Pb zircon analyses (Stern, Bateman, Morgan, Newell, and Peck, 1981), was called the Oakhurst pluton. This name was abandoned in the summary by Bateman (1992) because good intrusive contacts with surrounding tonalite outcrops could not be found in the field. A

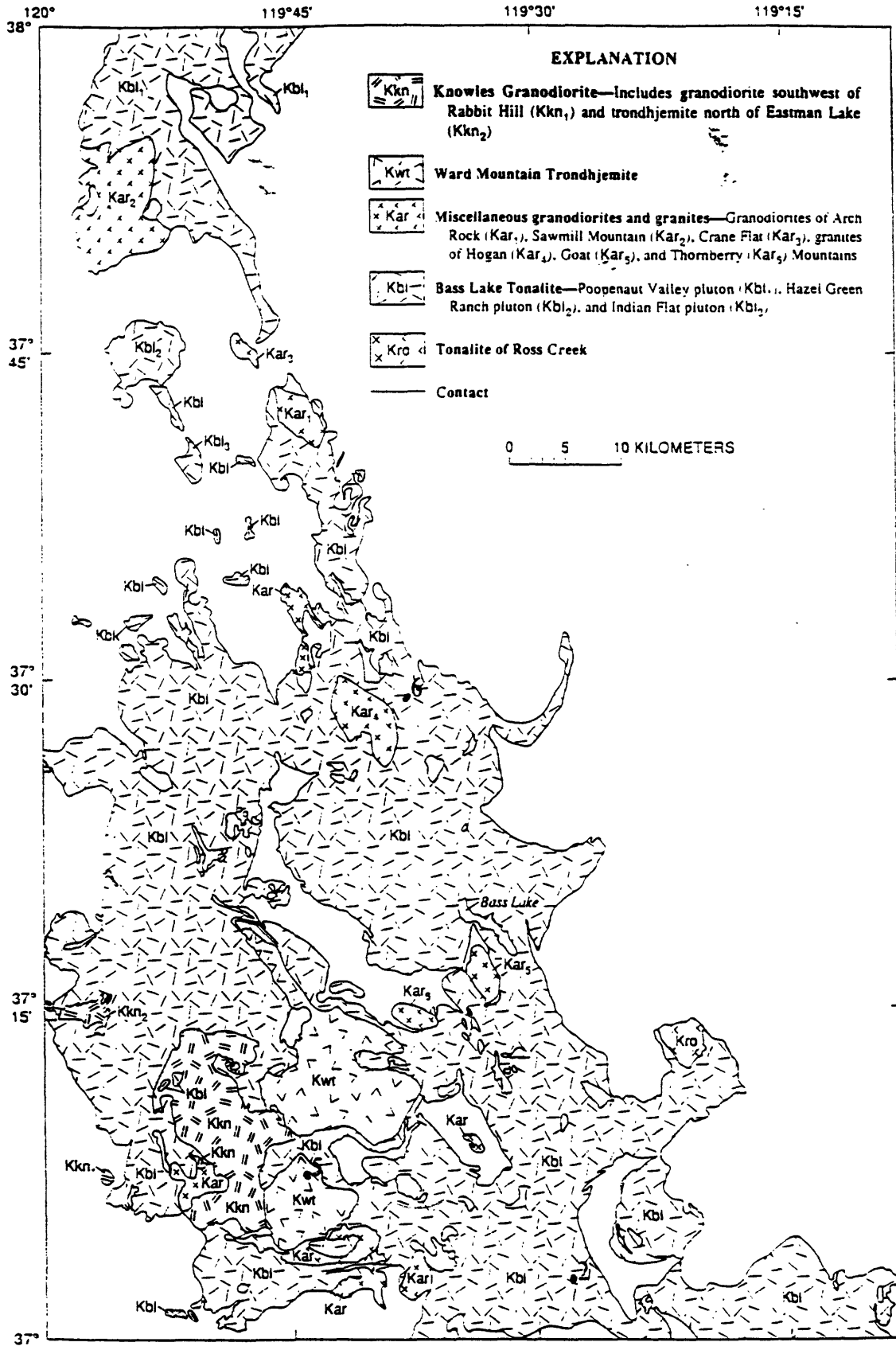

Figure 6. Generalized geology of the Fine Gold Intrusive Suite (modified from Bateman, 1992). The locations of field trip stops 2, 5, and 6 are shown as numbered dots.

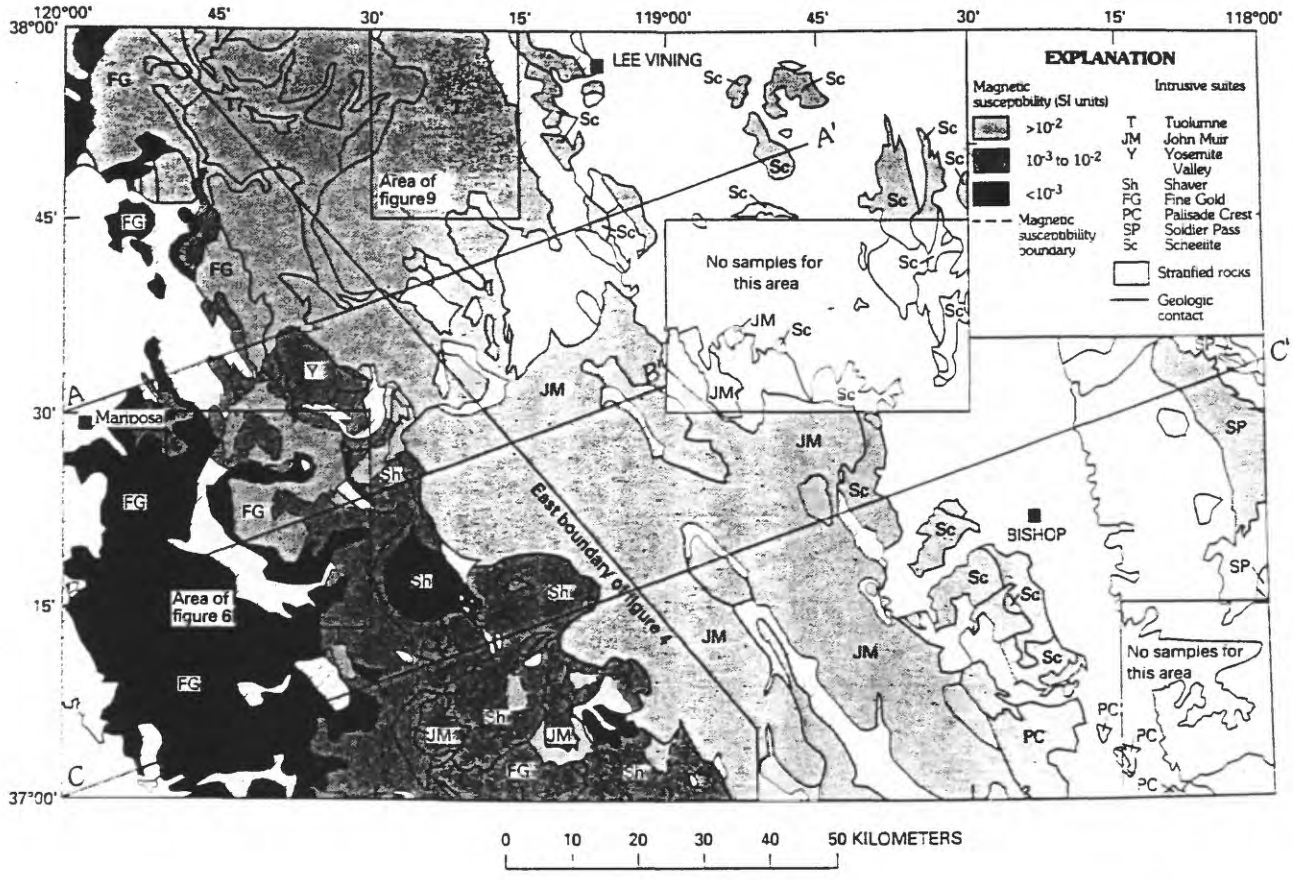

Figure 7. Generalized pre-Tertiary geologic map of Mariposa 1° by 2° quadrangle showing intrusive suites and general distribution of magnetic susceptibility values of the plutonic rocks (modified from Bateman and others 1991).

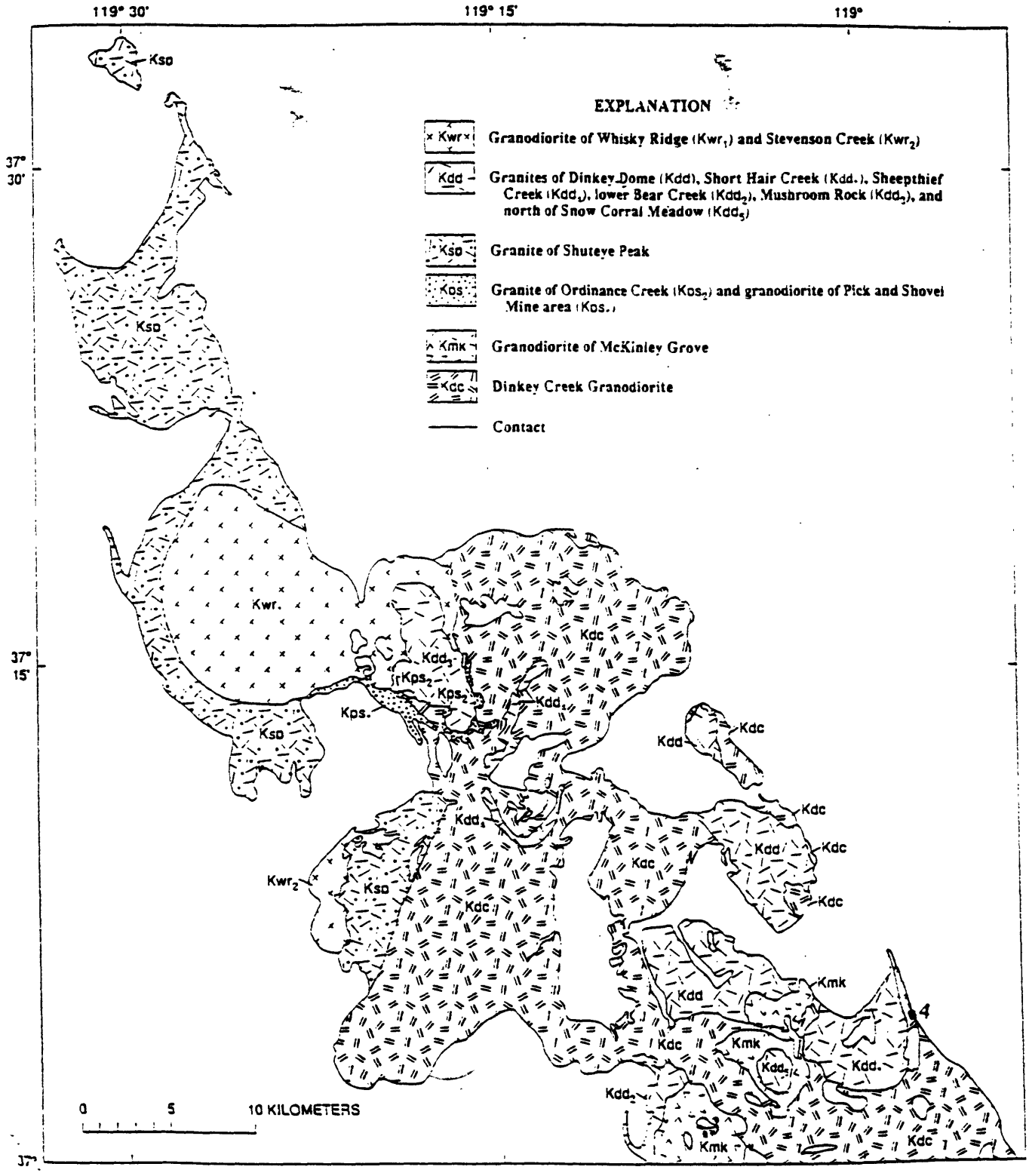

Figure 8. Generalized geology of the Shaver Intrusive Suite (modified from Bateman, 1992). The locations of field trip stops 3 and 4 are shown by numbered dots.

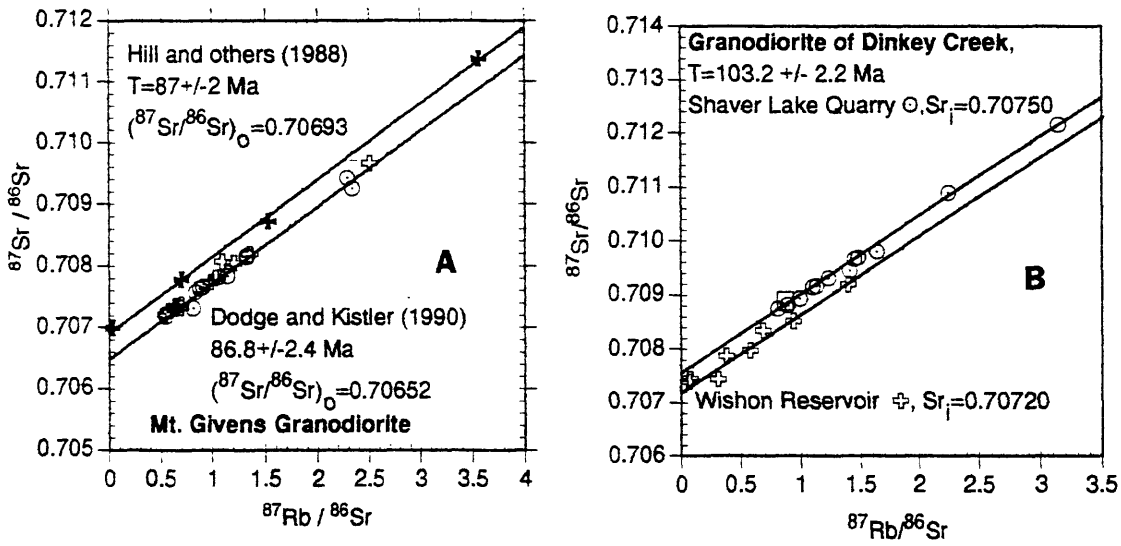

Figure 9. Strontium evolution, isochron diagrams for the Mount Givens Granodiorite (A.) and the Dinkey Creek Granodiorite (B.) for samples collected from two different localities in each body. The data of Hill and others (1988) is for a whole-rock, mineral isochron for a sample of the Mount Givens Granodiorite collected near Florence Lake to the north of the Courtright intrusive zone. The data of Dodge and Kistler (1990) for the Mount Givens Granodiorite is from whole-rock hosts, mafic inclusions, and aggregates from samples collected at Courtright intrusive zone. The data for the Dinkey Creek Granodiorite (Dodge and Kistler, 1990) are for whole-rock hosts, mafic inclusions, and aggregates from samples collected from a quarry near the town of Shaver Lake and from exposures near the Wishon Reservoir to the west and south, respectively, of the Courtright intrusive zone.

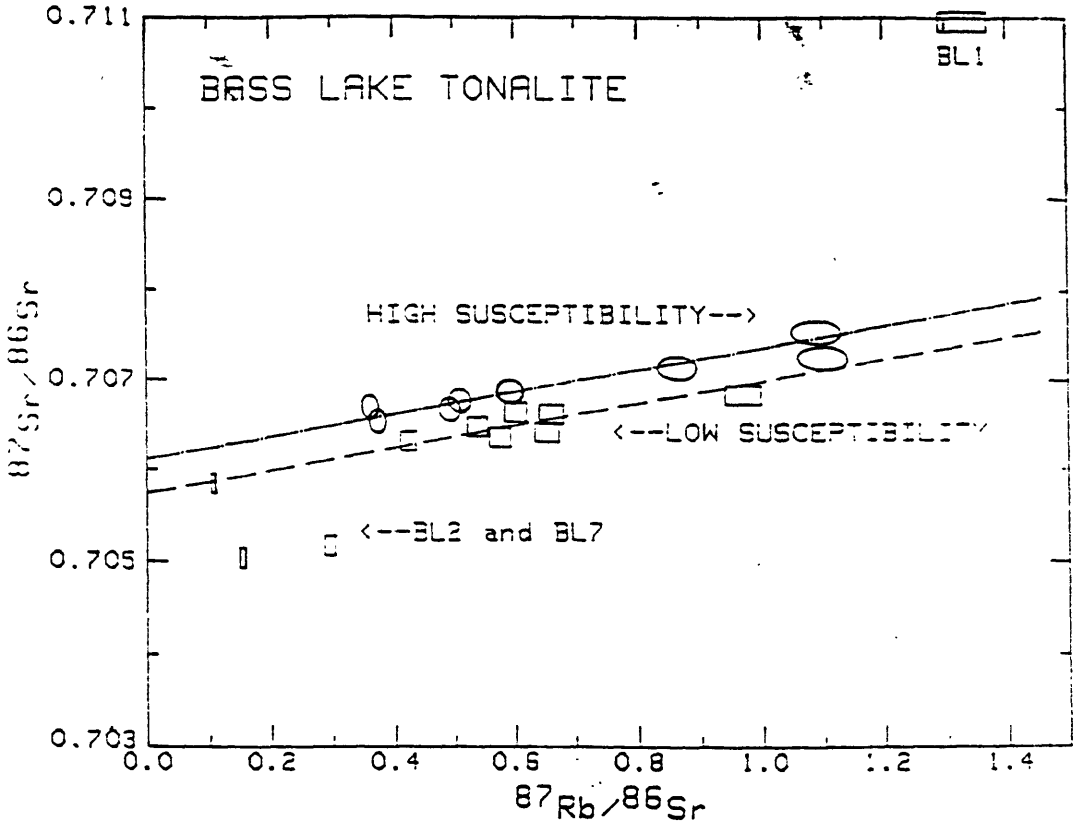

Figure 10.Strontium evolution diagram for whole-rock specimens of Bass Lake Tonalite collected along Hwy. 41 to the north of the Coarse Gold roof pendant. Variation in magnetic susceptibility correlated with the variation in initial $^{87}Sr/^{86}Sr$ values of the rocks. Rocks with high susceptibility (magnetite bearing) or low susceptibility (ilmenite bearing) had initial $^{87}Sr/^{86}Sr$ values greater than or less than 0.7060, respectively. Specimen BL1 is a quartzite at the contact between the intruded metamorphosed sedimentary rocks and the pluton.

regional study of magnetic susceptibility of granitoid rocks in the central Sierra Nevada by Bateman, Kistler and Dodge (1991), however, showed extreme variation in susceptibility in this body that correlated well with variations in initial $^{87}Sr/^{86}Sr$ isotopic ratios (Figure 10). These data indicate that the Oakhurst pluton is made up of at least three isotopically and magnetically discrete facies of tonalite that so far have resisted definition by field mapping. Their isotopic differences, however, reflect derivation from different sources and these similar tonalitic units are actually different intrusions.

Continue north on Hwy 41, passing through Oakhurst to the final Bass Lake Tonalite stop, one mile north of Fish Camp and east of Summerdale Campground.

55.9 (32.6) Stop #6. Bass Lake Tonalite

The roadcut exposure on the east (right) side of Hwy 41 is of biotite, hornblende tonalite with a few mafic inclusions. We are in the transition area to magnetite-series rocks (Figure 7) and magnetic susceptibility varies from about 4 to 9 units on the Kappa meter. Susceptibility of the mafic inclusions varies from 1.6 to 2.5 units with an average of about 2.3 units.

Continue north on Hwy 41 from Stop #6 into Yosemite National Park (about 0.6 mi.)

56.5 (0.6) Yosemite National Park. General statement.

On the basis of his field mapping, Calkins (1930) separated the granitoid rocks of the Yosemite Valley area into two groups or "series": an older, biotite granite series now called the intrusive suite of Yosemite Valley and a younger, biotite-hornblende-bearing, Tuolumne Intrusive Series (now called Tuolumne Intrusive Suite). The former is comprised of four main rock units from older to younger, the El Capitan Granite, the granite of Rancheria Mountain, the leucogranite of Ten Lakes, and the Taft Granite (Figure 11). Units of the younger suite from oldest to youngest are, the granodiorite of Yosemite Creek, Sentinel Granodiorite, granodiorite of Kuna Crest, Half Dome Granodiorite, Cathedral Peak Granodiorite, and Johnson Granite Porphyry (Figure 12). The main, two-fold, separation into two series (now intrusive suites using the modern stratigraphic code) by Calkins (1930) has stood the test of time. However, geochronologic and isotopic-tracer studies indicate that the boundaries between rock units defined by mapping in the Tuolumne Intrusive Suite do not always mark the major compositional and temporal breaks in the intrusive sequence. These include *potassium-argon dating* (Curtis, Evernden, and Lipson, 1958; Kistler and Dodge, 1966, Evernden and Kistler, 1970), *U-Pb dating* of zircon (Stern and others, 1981) and sphene (Wooden, written communication, 1994; Fleck and Kistler, 1994), *rubidium-strontium* whole-rock and mineral isochrons (Kistler, Chappell, Peck, and Bateman, 1986; Fleck and Kistler, 1994), *$^{40}Ar/^{39}Ar$ incremental-heating* ages of hornblende, biotite, and potassium-feldspar (Fleck and Kistler, 1994), and *isotopic studies* of strontium, neodymium, lead, and oxygen (Kistler, Chappell, Peck, and Bateman, 1986; and additional stable isotopic data from this study, Table 2). As our trip crosses Yosemite National Park, we will examine and discuss a number of these mapped boundaries, which range from well defined to gradational, cryptic, and unrecognized.

Continue north on Hwy 41 from the south boundary of Yosemite National Park to Quinquapin, the junction of Hwy 41 with the Glacier Point Road, 18.2 mi. from Stop #6. Turn right (east) on Glacier Point Road and drive 15.1 mi. to the Washburn Point turnout.

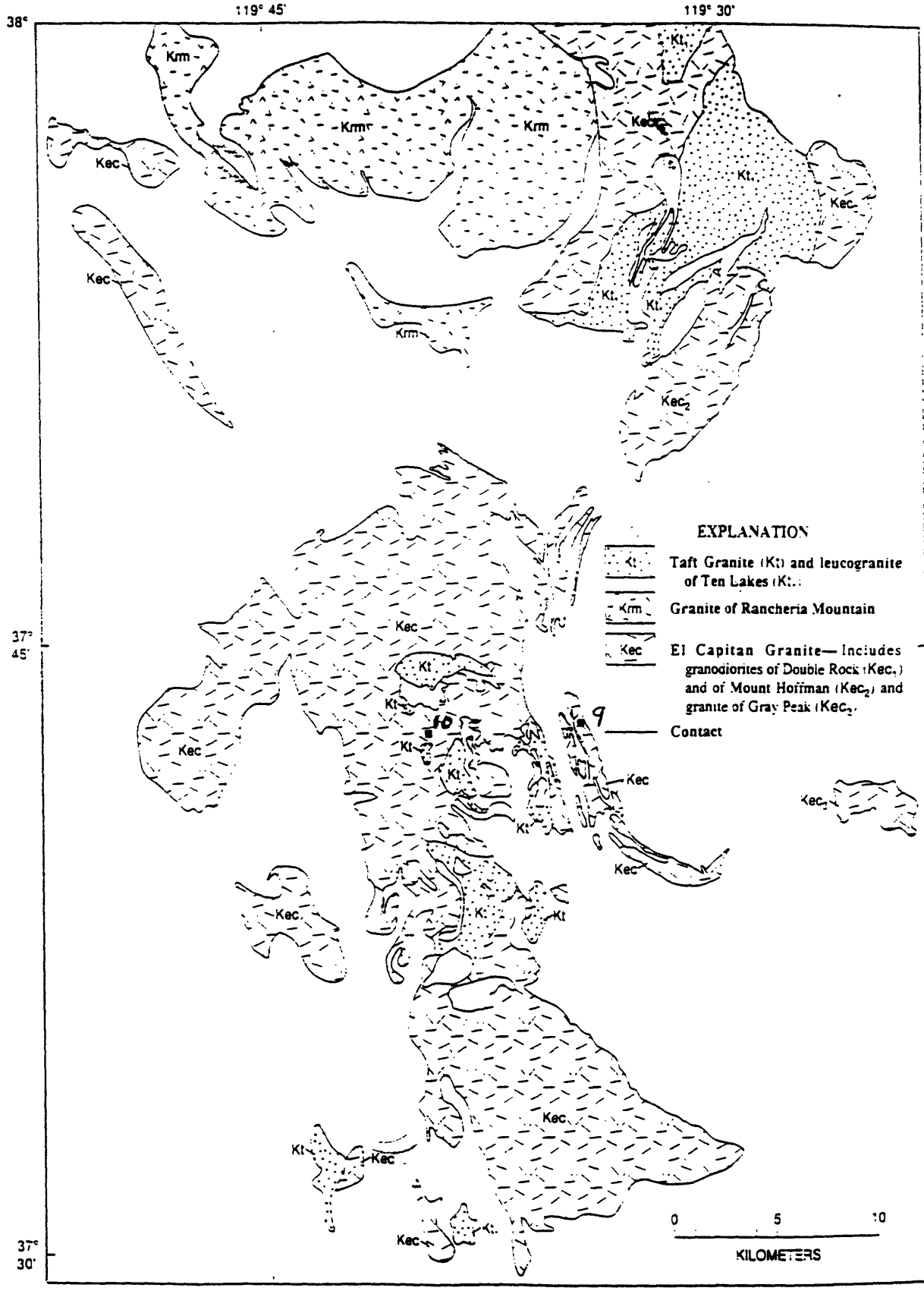

Figure 11. Generalized geology of the intrusive suite of Yosemite Valley (modified from Bateman, 1992). The location for field trip stops 9 and 10 are shown by numbered dots.

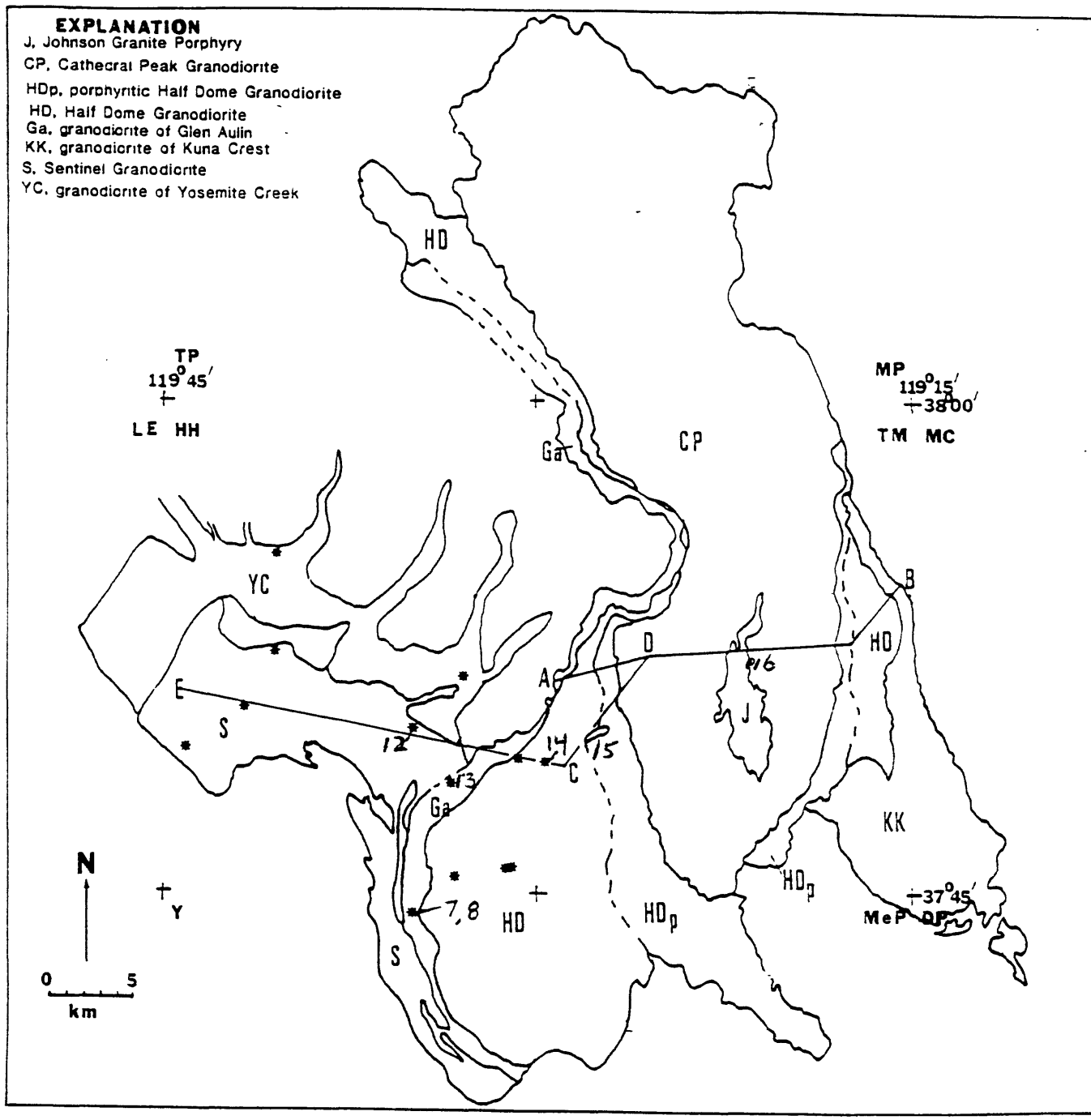

Figure 12. Map of the Tuolumne Intrusive Suite (modified from Kistler and others, 1986). Sample Traverses: AB and CD (Bateman and Chappell, 1979) and EC (Kistler 1974). Asterisks are specimen locations in the Hetch Hetchy quadrangle (Kistler, 1974). All whole-rock isotopic data from specimens along these traverses is summarized in Table 2. Field trip stops 7, 8, 12, 13, 14, 15, and 16 are shown by numbered dots.

Table 2. Strontium, oxygen, hydrogen, and neodymium isotopic data for whole-rock specimens of the Tuolumne Intrusive Suite along traverses A-B, C-D, and E-C on Figure 12. Samples are arranged consecutively from west to east along each traverse. Hydrogen values are reported in per mil relative to PDB belemnite. The reductions of other isotopic values are defined in Table 1. Rock units: KK, granodiorite of Kuna Crest; GP, tonalite of Glacier Point; HDo, outer Half Dome Granodiorite; HDi, inner Half Dome Granodiorite; HDapl, inner Half Dome aplite; CPo, outer Cathedral Peak Granodiorite; CPi, inner Cathedral Peak Granodiorite; J, Johnson Granite Porphyry.

Field No., unit		Rb(ppm)	Sr(ppm)	Rb/Sr	$^{87}Rb/^{86}Sr$	$^{87}Sr/^{86}Sr$	$(^{87}Sr/^{86}Sr)_o$	$\delta^{18}O$	δD	$\varepsilon_{Nd}T$
TMc-122	Ga	88	616	0.143	0.413	0.70650	0.70598			
Z51	Ga	108	574	0.188	0.544	0.70656	0.70587	+7.1	-73.4	
Z52	Ga	102	551	0.185	0.535	0.70641	0.70573	+7.0		
Z53	Ga	140	507	0.276	0.799	0.70692	0.70591	+7.1	-99.5	-3.9
Z54	HDo	134	478	0.280	0.811	0.70675	0.70546	+7.6	-74.7	
Z55	HDo	131	451	0.306	0.885	0.70723	0.70604	+7.6		
Z56	HDo	127	412	0.308	0.892	0.70719	0.70606	+7.8	-77.8	
Z57	HDo	114	509	0.224	0.648	0.70692	0.70612			
Z58	HDi	141	462	0.305	0.883	0.70744	0.70636	+8.0		-5.3
Z59	HDi	153	397	0.385	1.115	0.70769	0.70633	+7.9	-81	
Z60	HDi	138	491	0.281	0.813	0.70733	0.70634	+8.6		
Z61	CPo	129	658	0.196	0.567	0.70712	0.70643	+7.6		
Z62	CPo	104	701	0.148	0.429	0.70695	0.70643	+7.6	-77.9	
Z63	CPo	135	582	0.232	0.671	0.70729	0.70647			-5.2
Z35	CPo	129	710	0.182	0.526	0.70708	0.70644	+7.5	-76.2	
Z10	CPi	134	663	0.202	0.585	0.70709	0.70639	+8.3		
Z36	CPi	127	641	0.198	0.573	0.70701	0.70633	+8.3		
Z11	CPi	137	621	0.221	0.638	0.70716	0.70640			
Z37	CPi	132	585	0.226	0.653	0.70712	0.70634	+7.7		
Z38	CPi	165	525	0.314	0.909	0.70765	0.70657	+8.2		
Z39	J	189	277	0.682	1.975	0.70907	0.70681	+8.4	-84	
Z18	J	158	484	0.326	0.944	0.70776	0.70668	+8.3	-80.7	-8
Z19	J	207	301	0.688	1.99	0.70906	0.70679	+8.8		
Z12	CPi	150	369	0.407	1.176	0.70788	0.70648	+8.1		
Z40	CPi	143	628	0.228	0.659	0.70713	0.70634	+8.0	-80.4	
Z13	CPi	131	609	0.215	0.622	0.70710	0.70636	+7.7		
Z14	CPi	133	648	0.205	0.594	0.70706	0.70635	+8.2	-84.5	
Z41	CPo	107	695	0.154	0.445	0.70704	0.70650	+7.8	-82.7	
Z42	CPo	114	699	0.163	0.472	0.70697	0.70639	+7.7	-82	
Z43	HDo	107	579	0.185	0.535	0.70679	0.70611	+8.0	-83.4	
Z16	HDo	163	380	0.429	1.241	0.70760	0.70603	+7.8		
Z44	KK	123	511	0.239	0.691	0.70683	0.70596	+7.3	-73.6	
Z45	KK	113	563	0.201	0.581	0.70678	0.70605	+7.6	-70.5	
Z46	KK	119	482	0.247	0.714	0.70679	0.70589	+7.6		
Z47	KK	102	545	0.187	0.541	0.70654	0.70586	+6.6	-106.6	
End traverse A-B										
Z5	HDi	146	436	0.335	0.969	0.70745	0.70629	+7.9	-84.4	
Z23	HDi	130	526	0.247	0.715	0.70707	0.70620	+7.9		
Z6	HDi	114	578	0.197	0.571	0.70692	0.70622	+7.3		
Z24	HDi	121	555	0.218	0.631	0.70707	0.70630			
Z25	HDi	114	568	0.201	0.581	0.70696	0.70625			
Z26	HDi	136	510	0.267	0.771	0.70722	0.70628	+8.0		
Z7	HDi	110	688	0.160	0.463	0.70682	0.70625			
Z27	HDi	149	413	0.361	1.044	0.70757	0.70630			
Z28	HDi	127	572	0.222	0.642	0.70714	0.70636			
Z8	CPo	117	633	0.185	0.535	0.70696	0.70631	+7.5	-85.7	
Z29	CPo	128	631	0.203	0.587	0.70726	0.70654			
Z30	CPo	118	641	0.184	0.533	0.70709	0.70644			
Z31	CPo	100	709	0.141	0.408	0.70698	0.70648			
Z32	CPo	106	689	0.154	0.445	0.70699	0.70645			
Z23	CPo	113	715	0.158	0.457	0.70709	0.70653			
Z9	CPo	127	668	0.190	0.55	0.70710	0.70643	+7.7	-92.6	

Table 2 continued

Field No., unit		Rb(ppm)	Sr(ppm)	Rb/Sr	$^{87}Rb/^{86}Sr$	$^{87}Sr/^{86}Sr$	$(^{87}Sr/^{86}Sr)_o$	$\delta^{18}O$	δD	$\varepsilon_{Nd}T$
Z34	CPo	128	618	0.207	0.599	0.70713	0.70640			
Z20	CPo	126	667	0.189	0.547	0.70714	0.70647			
End traverse C-D										
Z15	KK	101	592	0.171	0.494	0.70628	0.70566			
FD-13	GP	60.2	621	0.100	0.28	0.70612	0.70580	+6.4		
K46-64	GP	120	486	0.247	0.715	0.70654	0.70564			-3.2
H38-69	HDo	147	363	0.405	1.172	0.70762	0.70610	+8.0		
H42-69	HDi	149	381	0.391	1.131	0.70758	0.70620	+8.2		
H41-69	HDapl	205	180	1.139	3.295	0.71019	0.70620	+8.3		
12	HDo	124	391	0.317	0.917	0.70720	0.70604	+8.0		
13	HDo	124	470	0.263	0.761	0.70700	0.70607	+8.0		
S-Sr-T1	CPi	155	592	0.261	0.755	0.70740	0.70650	+8.2		-6.3
H48-69	YC	79.1	517	0.153	0.443	0.70730	0.70673			
K29-66	YC	69.5	498	0.140	0.404	0.70744	0.70692			
K5-64	S	56.1	747	0.075	0.217	0.70680	0.70658			-4.5
K7-64	S	70.5	687	0.103	0.298	0.70677	0.70639			
K37-6	S	62.3	684	0.091	0.263	0.70706	0.70672			-5.9
K40-64	S	97.6	498	0.196	0.567	0.70740	0.70668			
End traverse		E-C								

89.2 (32.7) Stop #7. Washburn Point.

Outcrops of hornblende biotite tonalite around the parking area at Washburn Point are now referred to the tonalite of Glacier Point. This unit was part of the original Sentinel Granodiorite of Calkins (1930), the outer and oldest unit of his Tuolumne intrusive series. This unit is now subdivided on the basis of subsequent mapping, geochemistry, and isotopic studies into three discrete entities, the granodiorite of Yosemite Creek, the Sentinel Granodiorite, and granodiorite of Kuna Crest, in order from oldest to youngest. The granodiorite of Kuna Crest is subdivided further and includes a more mafic phase at this outcrop, the tonalite of Glacier Point (Figure 12). Curtis, Evernden, and Lipson (1958) published a K-Ar date on biotite from this unit at 86.4 Ma. Kistler and Dodge (1966) dated biotite, hornblende, orthoclase, plagioclase, and augite at 91.7, 92.2, 90.2, 83.0, and 80.0 Ma, respectively, by the potassium-argon technique from a specimen collected from this locality. A whole-rock, biotite, plagioclase, K-feldspar, hornblende, and apatite Rb-Sr isochron gave an age of 84.8 ±0.8 Ma with an initial $^{87}Sr/^{86}Sr = 0.70580$ (Kistler and others, 1986). $^{40}Ar/^{39}Ar$ incremental-heating plateau ages for biotite and hornblende from the same sample are 87.59±0.47 Ma and 88.98±0.72 Ma, respectively (Fleck and Kistler, 1994). Stern and others (1981) reported a slightly discordant U-Pb zircon date with a $^{206}Pb/^{238}U$ age of 88 Ma for a specimen of this unit collected near May Lake to the north of here on the north side of Yosemite Valley.

Continue on the Glacier Point Road another 0.7 mi. to its end in the parking area at Glacier Point. We will observe additional exposures of the tonalite of Glacier Point as we hike to the end of the point for impressive views of glacial features in Yosemite Valley.

89.9 (0.7) Stop #8. Glacier Point.

Glacier Point is the most famous overlook of Yosemite Valley and also presents a view of some of the higher elevation back-country of Yosemite National Park. To the northeast is the glacially carved face of Half Dome and flow from Yosemite Creek exits its hanging valley at the top of Yosemite Falls to the north-northwest. The rock unit exposed here is the tonalite of Glacier Point, nearly identical to exposures just examined at Washburn Point (Figure 12). Note the abundance of coarse hornblende and the generally dark-gray appearance of this rock, the only tonalite within the generally granodioritic Tuolumne Intrusive Suite.

We will return to the vehicles and leave Glacier Point, climbing slowly back up the grade in the Glacier Point Road to the Sentinel Dome parking area on the north (right) side of the road (about 2.4 mi.).

92.3 (2.4) Stop #9. Sentinel Dome; El Capitan Granite/Sentinel Granodiorite contact.

Glacier Point Road trends SW-NE past the Sentinel Dome parking area. In the road cuts along the opposite (southeast) side of the road we can obtain a summary of the geologic story we get on our hike out to Sentinel Dome. On the northeast end of the road cut the El Capitan Granite of the Intrusive Suite of Yosemite Valley with large, gray-appearing "eyes" of quartz is practically undeformed. Moving southwest along the road cut, we begin to see zones of mafic, hornblende biotite granodiorite cutting through and incorporating the granite. At the southwest end of the road cut we see nearly massive hornblende-bearing Sentinel Granodiorite of the Tuolumne Intrusive Suite. Starting north along the trail to Sentinel Dome, we see Sentinel Granodiorite intruding the El Capitan Granite that occurs as a multitude of inclusions in the granodiorite. All proportions of the two units may be found in the 1.1 mi. hike to the top of Sentinel Dome. The domical edifice itself is almost entirely El Capitan Granite, which contains older mafic enclaves in places. Where interactions occur with Sentinel Granodiorite, however, the more mafic Sentinel is always intrusive, although the Sentinel may appear almost gradational in places. It is this variable nature of the contact that we wish to emphasize here, because not only is the mafic phase intruding the leucocratic phase, but the difference in age between the phases is not apparent from the small-scale intrusive relationships. A specimen of El Capitan Granite from Sentinel Dome is one of eight samples on a Rb-Sr whole-rock isochron for the biotite granite series of Yosemite Valley that yields an age of 101.5 Ma and an initial $^{87}Sr/^{86}Sr = 0.70645$ (Figure 13). DePaolo (1981) reports an $\varepsilon_{Nd}T = -3.9$ for a specimen of the El Capitan Granite. A U-Pb zircon date from the El Capitan Granite is 102.8 Ma (Stern and others, 1981). With an age of about 90 Ma for the Sentinel Granodiorite these ages define a 12 Ma age difference, whereas outcrop-scale exposures could be interpreted as indicating Sentinel intrusion during the late magmatic stage of El Capitan emplacement.

We return to the Sentinel Dome parking area and resume our trip southwestward on the Glacier Point Road back to Chinquapin (13.4 mi.). At Chinquapin turn right (north) on Hwy 41, traveling toward Yosemite Valley. After 6.8 mi. we reach the west end of Wawona Tunnel, a 0.8 mile tunnel through the last ridge between us and the valley. Stop at the east-end vista point turnout.

113.4 (21.1) Stop #10. Discovery View; View Stop at East-End Wawona Tunnel.

The rock at the east end of Wawona Tunnel and at the viewpoint is El Capitan Granite with inclusions of diorite to gabbro. The stop here is a photo opportunity, and a chance to look at the Park Service signs describing the Yosemite Valley panorama. Leave the view stop and proceed to Yosemite Lodge (7.0 mi.), passing El Capitan (seen through the trees on the left side of the bus) and Bridalveil Fall (on the right) enroute.

Day 3. Yosemite Valley to Mammoth Lakes, California.

0.0 (0.0) Leave Yosemite Lodge traveling west on the Northside Drive (5.7 mi. from Yosemite Lodge) to the junction of Hwy 140 (to El Portal and Mariposa) and the New Big Oak Flat Road (to Hwy 120). Turn right on the New Big Oak Flat Road and proceed

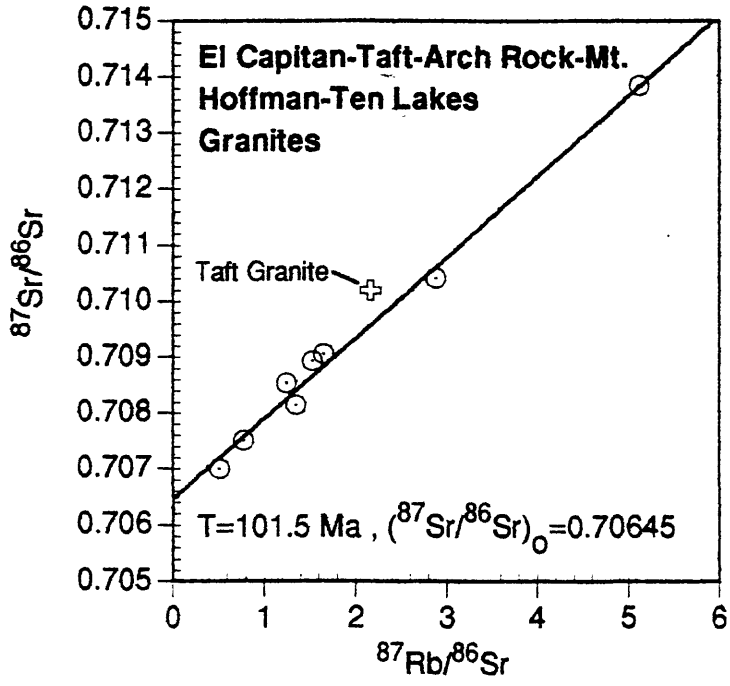

Figure 13.Rb-Sr whole-rock isochron plot for specimens of intrusive suite of Yosemite Valley (El Capitan, Taft, Arch Rock, Hoffman, and Ten Lakes plutons). The specimen of Taft Granite is not included in the isochron regression.

another 9.6 mi. up out of Yosemite Valley to Crane Flat, the junction with Hwy 120. Turn right (eastbound) on Hwy 120 toward Tioga Pass.

19.0 (19.0) Before we get to Stop #11 on Hwy 120, we pass the turnout at Gin Flat (3.7 mi. east on Hwy 120), where a correlative of the Bass Lake Tonalite, the tonalite of Poopenaut Valley (Dodge and Calk, 1987) represents the mafic, diorite-tonalite sequence we observed in the Sierran foothills before entering Yosemite National Park. It is a medium-grained biotite-hornblende tonalite that ranges locally from granodiorite to quartz diorite. It contains subhedral to euhedral mafic minerals and has a color index that ranges widely from about 7 to nearly 30, but generally averages 20. It is locally sheared, and is commonly more felsic where sheared than elsewhere. Initial $^{87}Sr/^{86}Sr$ values in this unit exhibit a wide range, from 0.7045 to 0.7063 (Kistler, unpublished data). From a specimen collected at Gin Flat, Dodge and Calk (1986) report a U-Pb zircon age of 117.5 Ma and K-Ar ages of 114.3 Ma (hornblende) and 100.6 Ma (biotite) . A contact with the El Capitan Granite is only 500 meters away to the southeast, and the biotite K-Ar date reflects the time of emplacement and cooling of that pluton.

Continue eastward on Hwy 120 past Gin Flat to the turnout several hundred feet east of the bridge over the South Fork of the Tuolumne River (7.4 mi. east of Crane Flat Jct. and 22.7 miles from Yosemite Lodge).

22.7 (3.7) **Stop #11. South Fork of the Tuolumne River.**

The rock is the quartz diorite of South Fork of Tuolumne River (Kistler, 1973) and is continuous with the quartz diorite of Aspen Valley (Dodge and Calk, 1987). The rock is undated at this locality, but it is probably a facies of the Early Cretaceous tonalite of Poopenaut Valley. The pluton is comprised of medium-grained biotite-hornblende tonalite to quartz diorite. It contains subhedral to euhedral mafic minerals and has a color index of about 20. It is locally sheared, and where sheared more felsic than elsewhere. Assuming and age of 118 Ma for this pluton, it has an initial $^{87}Sr/^{86}Sr = 0.7056$ (Kistler, unpublished data).

From Stop #11, continue to the east on Hwy 120 for 10.4 miles to just east of the Dark Hole. Pull out on the right side of the road.

33.1 (10.4) **Stop #12. Yosemite Creek/Sentinel Granodiorite Contact.**

Exposures in the road cut on the east (left) side of Hwy 120 that include a contact within the Tuolumne Intrusive Suite between the granodiorite of Yosemite Creek and the Sentinel Granodiorite. This is one of the bases for subdivision of the original Sentinel Granodiorite of Calkins (1930), but as close examination demonstrates, the contact is not immediately obvious. The granodiorite of Yosemite Creek is characterized by mafic inclusions that are flat and subhorizontal within the 20 meters north of the contact. The contact with the Sentinel Granodiorite is subvertical and truncates this subhorizontal foliation in the older granodiorite. These two plutons that were mapped as part of the same unit by Calkins (1930) have not been dated radiometrically, but both intrude the 102-Ma-old El Capitan Granite. Because they are hornblende bearing, both are considered by us to be part of the Tuolumne Intrusive Suite. The oldest dated unit of this suite is the tonalite of Glacier Point at 90 Ma, visited in Stops 7 and 8. The granodiorite of Yosemite Creek is predominantly biotite-hornblende quartz diorite, that is coarse grained, dark-gray, and grades to granodiorite. Locally, this pluton is porphyritic with white phenocrysts of plagioclase. Its average color index is about 15, but ranges from 7 to 35. Two specimens of the body have initial $^{87}Sr/^{86}Sr$ values of 0.7067 and 0.7069 assuming an age of 92 Ma (Kistler,

Chappell, Peck, and Bateman, 1986). The Sentinel Granodiorite is also coarse-grained, dark-gray, and biotite-hornblende granodiorite. Its color index averages about 15. Assuming this pluton is the same age as the granodiorite of Yosemite Creek, four specimens have initial $^{87}Sr/^{86}Sr$ values that range from 0.7064 to 0.7067 and two of these have $\varepsilon_{Nd}T$ values of -4.5 and -5.9 (Kistler, Chappell, Peck, and Bateman, 1986, Table 2). Table 2, summarizes all of the whole-rock isotopic data for Tuolumne Suite rocks.

These rocks are in the magnetite-series with susceptibilities that range from about 12 to 17 units, whereas mafic inclusions range from about 18 to 20 units.

Continue east on Hwy 120 for 6.4 miles to the parking area for the California red fir and lodge pole pine Life Zone exhibit, about 0.5 miles past Porcupine Flat.

39.5 (6.4) Stop #13. Tonalite of Glacier Point at Life-Zone Area.

The exposures of granitoid rock here are the tonalite of Glacier Point, similar to those we observed at Glacier Point itself, but perhaps a little finer grained. This unit represents the innermost of the three phases of Calkins' original Sentinel Granodiorite (Calkins, 1930). The rock is a dark-colored, foliated, fine-to medium-grained tonalite. The color index of the rock here is about 20, the initial $^{87}Sr/^{86}Sr = 0.7057$, and the $\delta^{18}O = +8$ per mil (Kistler, Chappell, Peck, and Bateman, 1986, Table 2). The magnetic susceptibility of the tonalite ranges from about 15 to 18 units.

The Life Zone exhibit is a nice display showing the different life-zones traversed as the elevation increases in the Sierra Nevada. Different species of trees characterize the different zones, and here the predominant trees are California red fir and lodge pole pine.

Resume travelling eastward on Hwy 120.

42.7 (3.2) At 3.2 miles east of Stop #13 (the life-zone display) the highway passes through a cross-section of a late Wisconsin (Wurm) glacial moraine. The faceting of boulders and the unsorted character of the deposit are clear as we drive along Hwy 120, cut through the moraine itself. Continue for an additional 1.8 miles to the Olmsted Point parking area.

44.5 (1.8) Stop #14. Olmsted Point, the Half Dome Granodiorite.

The biotite- and hornblende-bearing granodiorite exposed at Olmsted Point is the inner Half Dome Granodiorite that is medium-grained, equigranular, and characterized by euhedral hornblende prisms up to 1.5 cm, biotite books as much as 1 cm across, and conspicuous sphene (titanite). Exposures at Olmsted Point exhibit abundant mafic enclaves. The unit is continuous with exposures at Half Dome in Yosemite Valley, which is visible from some points at this viewpoint. The inner Half Dome has been recognized with our multi-method age profile across the Tuolumne Intrusive Suite (Fleck and Kistler, 1994). This facies of the Tuolumne suite is 86 Ma and a full 3 m.y. younger than the outer Half Dome Granodiorite and tonalite of Glacier Point (Figure 14). The contact between the inner and outer phases of the Half Dome Granodiorite has not been mapped, but it is marked in some areas by an aplite body mapped within the undifferentiated unit in the Hetch Hetchy quadrangle (Kistler, 1973). Inspection of the strontium isotopic data (Table 2) for the Half Dome Granodiorite within the concentrically-zoned western portion of the Tuolumne suite (Kistler, Chappell, Peck, and Bateman, 1986) relative to the age data reported by Fleck and Kistler (1994) shows a geographically-correlated change in initial $^{87}Sr/^{86}Sr$ values from 0.7055-0.7061 in the older, outer unit to 0.7062- 0.7064 for the younger, inner unit that

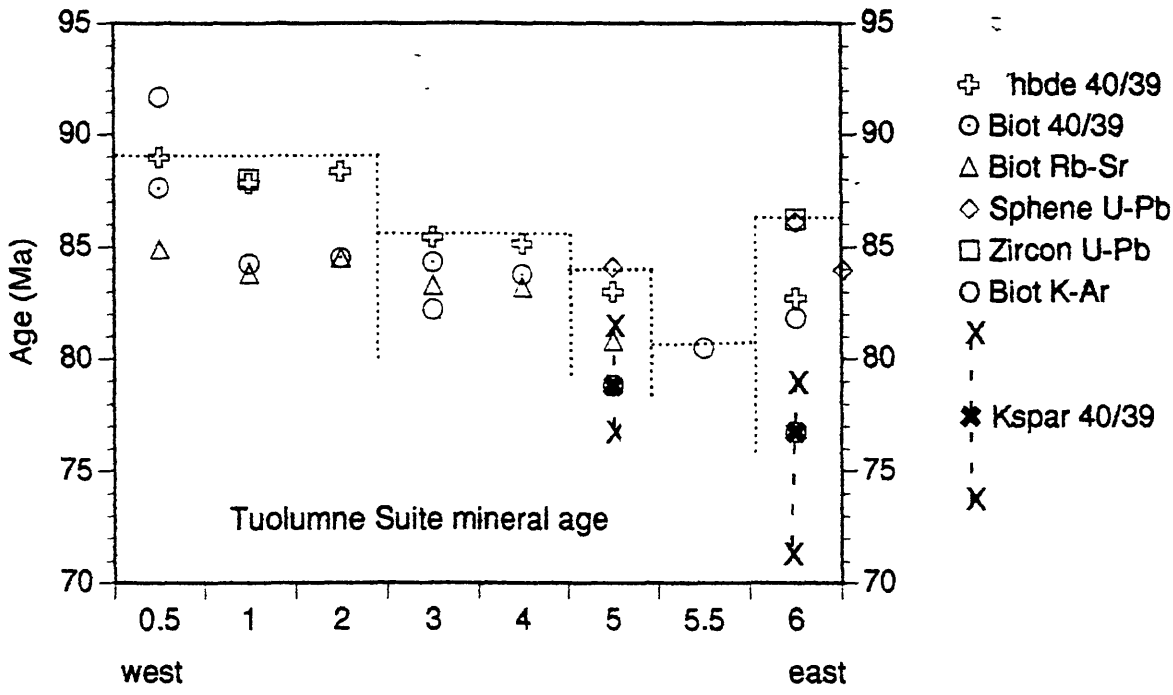

Figure 14. Multiple technique and mineral age-profile along traverse AB of Figure 12 except the westernmost data are from sample FD13 at Washburn Point (field trip stop 7). The x--x--x line for Kspar $^{40}Ar/^{39}Ar$ plot the minimum and maximum ages determined during argon release that did not yield a plateau. The central (x) is the calculated total gas age for these minerals.

coincides with the age discontinuity. The two specimens investigated from this locality (Z23, Z6, Table 2) have initial $^{87}Sr/^{86}Sr = 0.7062$ and $\delta^{18}O = +7.3$ and +7.9.

Continue east on Hwy 120 for 2.2 miles to the Tenaya Lake picnic area. The vehicles will disembark passengers for a 0.5 mile walking traverse along Hwy 120 on the north side of Tenaya Lake to examine exposures of the innermost part of the Half Dome Granodiorite and across the seemingly gradational contact with the outer part of the Cathedral Peak Granodiorite. Water and restroom facilities are normally available in the picnic grounds We will rejoin the vehicles at the second turnout to the east along Tenaya Lake.

46.7 (2.2) Stop #15. Tenaya Lake Picnic Grounds, Half Dome/Cathedral Peak contact.

We begin our traverse along Tenaya Lake in equigranular granodiorite of the Half Dome Granodiorite, as we walk eastward on the north side of the highway, facing traffic. As we continue eastward, we begin to see K-feldspar megacrysts in the granodiorite, but no other compositional or textural change is obvious. We proceed and see a completely gradational contact between equigranular and megacrystic granodiorite. The gradational contact between the two rock types resulted in Calkins (1930), Bateman and Chappell (1979), and Bateman, Kistler, Peck, and Busacca (1983) referring to the megacrystic rock as the porphyritic facies of the Half Dome Granodiorite. Age results (Fleck and Kistler, 1994; Figure 14) show the two rock types to be the same age at 86 Ma, but chemical (Bateman and Chappell, 1979) and isotopic differences between the two textural variants indicate they are from entirely different magma batches (Figure 15; Kistler, Chappell, Peck, and Bateman, 1986). Furthermore, the megacrystic phase is identical in chemical and isotopic characteristics to the outer part of the pluton mapped as Cathedral Peak Granodiorite (Kistler, Chappell, Peck, and Bateman, 1986), the next younger unit of the Tuolumne Intrusive suite.

The medium-grained, porphyritic hornblende-biotite granodiorite exposed at Tenaya Lake has a seriate texture and K-feldspar megacrysts that increase in abundance eastward. A sharp contact occurs within the megacrystic rocks on Polly Dome about 1 km to the north that was considered by previous workers to be the outer margin of Cathedral Peak Granodiorite. The granodiorite to the east of the contact contains conspicuous blocky megacrysts of K-feldspar 2 to 5 cm across, whereas those in the unit to the west are commonly half that size. Because the rocks on either side of this mapped contact are identical with respect to chemical and isotopic characteristics (Kistler, Chappell, Peck, and Bateman 1986), we conclude that the contact represents only a surge of still-mobile magma in the interior of a solidifying magma body and that both megacrystic varieties should now be assigned to the outer Cathedral Peak Granodiorite.

As to analytical results along our traverse, specimens Z27 and Z28 (Table 2) are from the equigranular granodiorite (the Half Dome) and samples Z8 and Z29 represent the megacrystic variety (the Cathedral Peak). Average initial $^{87}Sr/^{86}Sr$ values are 0.7063 and 0.7064 in the equigranular and megacrystic granodiorites, respectively. Values of $\delta^{18}O$ and δD in megacrystic specimen Z8 are +7.5 per mil and -85.7 per mil, respectively.

47.2 **(0.5)** We board the vehicles waiting for us at the next turnout, ending our traverse in highly megacrystic granodiorite that we refer to the outer Cathedral Peak Granodiorite. We now continue east on Hwy 120 for 7.8 miles to Lembert Dome, passing the Tuolumne Meadows store and ranger station at 7.4 mi., and making a left turn into the parking area for the dome.

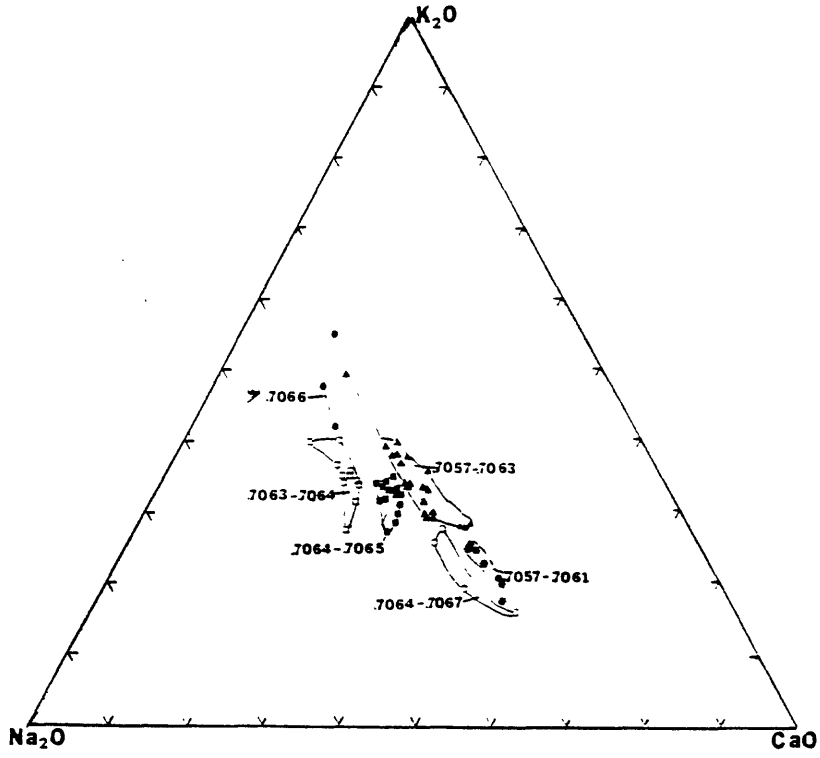

Figure 15. Triangular diagram showing K_2O, Na_2O, and CaO in rocks of the Tuolumne Intrusive Suite (modified from Kistler and others, 1986). Chemically coherent fields of different rock types with the range of initial $^{87}Sr/^{86}Sr$ are indicated: asterisks (0.7057-0.7061), tonalite of Glacier Point, tonalite of Glen Aulin and granodiorite of Kuna Crest; solid triangles (0.7057-0.7063), inner and outer parts of the Half Dome Granodiorite; solid squares (0.7064-0.7065), outer part of the Cathedral Peak Granodiorite; open squares (0.7063-0.7064), inner part of the Cathedral Peak Granodiorite; solid circles (>0.7066), Johnson Granite Porphyry;.open circles (0.7064-0.7067), Sentinel Granodiorite and granodiorite of Yosemite Creek.

55.0 (7.8) Stop #16. Cathedral Peak and Johnson Granite Porphyry at Lembert Dome.

Lembert Dome is a *roche moutonnée,* comprised of megacrystic, hornblende-bearing, biotite granodiorite with abundant glacial polish and striations. It is located near the center of the Tuolumne Intrusive Suite in Tuolumne Meadows and mapped as Cathedral Peak Granodiorite. The age profile of Fleck and Kistler (1994; Figure 14) shows this inner part of the Cathedral Peak Granodiorite to be 84 Ma in age, 2 m.y. younger than the outer part of the unit. The Cathedral Peak Granodiorite had already been separated into inner and outer parts on the basis of distinct isotopic and also chemical characteristics easily identified on a Na_2O, K_2O, CaO triangular plot (Kistler, Chappell, Peck, and Bateman, 1986, Figure 15). A contact between the two parts has not yet been identified in the field. Specimen Z40 (Table 2) of inner Cathedral Peak Granodiorite just to the east of this stop has initial $^{87}Sr/^{86}Sr = 0.70632$, and $\delta^{18}0$ and δD values of +8 per mil and -80.4 per mil, respectively.

In the grassy meadow to the west of Lembert Dome and south and west of the parking area, the Johnson Granite Porphyry is exposed as flat or nearly flat, bare patches of outcrop surrounded by the grasses of the meadow. The Johnson, the youngest and central body of the Tuolumne Intrusive Suite, is a fine-grained, porphyritic granite bordered by a network of dikes. The pluton contains sparse alkali feldspar megacrysts and miarolitic cavities. Mineral grains are commonly subhedral to anhedral, yielding a sucrosic or aplitic appearance. This unit is dated only by a single K-Ar determination on biotite at 80.5 Ma (Curtis, Evernden, and Lipson, 1958). Isotopically, three specimens of Johnson Granite Porphyry have $\delta^{18}O$ from +8.3 to +8.8 per mil, δD from -80.7 to -84 per mil, and initial $^{87}Sr/^{86}Sr$ from 0.7067 to 0.7068 (Table 2, Specimens Z39, Z18, and Z19). The specimen with initial $^{87}Sr/^{86}Sr = 0.7067$ yields $\varepsilon_{Nd}T = -8$ (Kistler, Chappell, Peck, and Bateman, 1986, Table 2).

From Lembert Dome, return to Hwy 120 and continue east for 7.0 miles to the east gate to Yosemite National Park at Tioga Pass. Leaving the National Park, continue eastward rapidly loosing elevation for an additional 4.1 miles to "camera viewpoint" turnout.

66.1 (11.4) Stop #17. Tioga Road Viewpoint, North Wall of Lee Vining Canyon.

Currently designated with a brown-colored sign of a camera, this popular view stop affords a grand overview of Lee Vining Canyon and the Mono Basin farther to the east. If the day is clear and valley haze is low, the White Mountains on the California-Nevada border will be visible on the horizon. Nearby, we see the mid-Cretaceous (96 Ma, K-Ar biotite, Evernden and Kistler, 1970) granite of Ellery Lake is exposed on the south wall of the canyon and the Late Triassic (216 Ma, initial $^{87}Sr/^{86}Sr = 0.7059$) granite of Lee Vining Canyon on both sides of the road. An unnamed tonalite also exposed along the canyon wall is dated at 97.5 Ma by K-Ar on hornblende (Evernden and Kistler, 1970). In Mono Basin we see the rhyolite domes and flows of the Quaternary Mono Craters that overlie a high desert valley floored by glacial lake deposits and the well-studied Bishop Tuff (760,000 years). Beyond the Mono Craters the Benton Range and Glass Mountain are visible in the middle distance (Figure 16).

Metamorphosed sedimentary rocks intruded by the Triassic and Cretaceous granitoid rocks are commonly seen as red-brown- to orange-weathering outcrops and consist of pelitic, quartzofeldspathic, siliceous, and minor calc-silicate hornfels. At the north end of

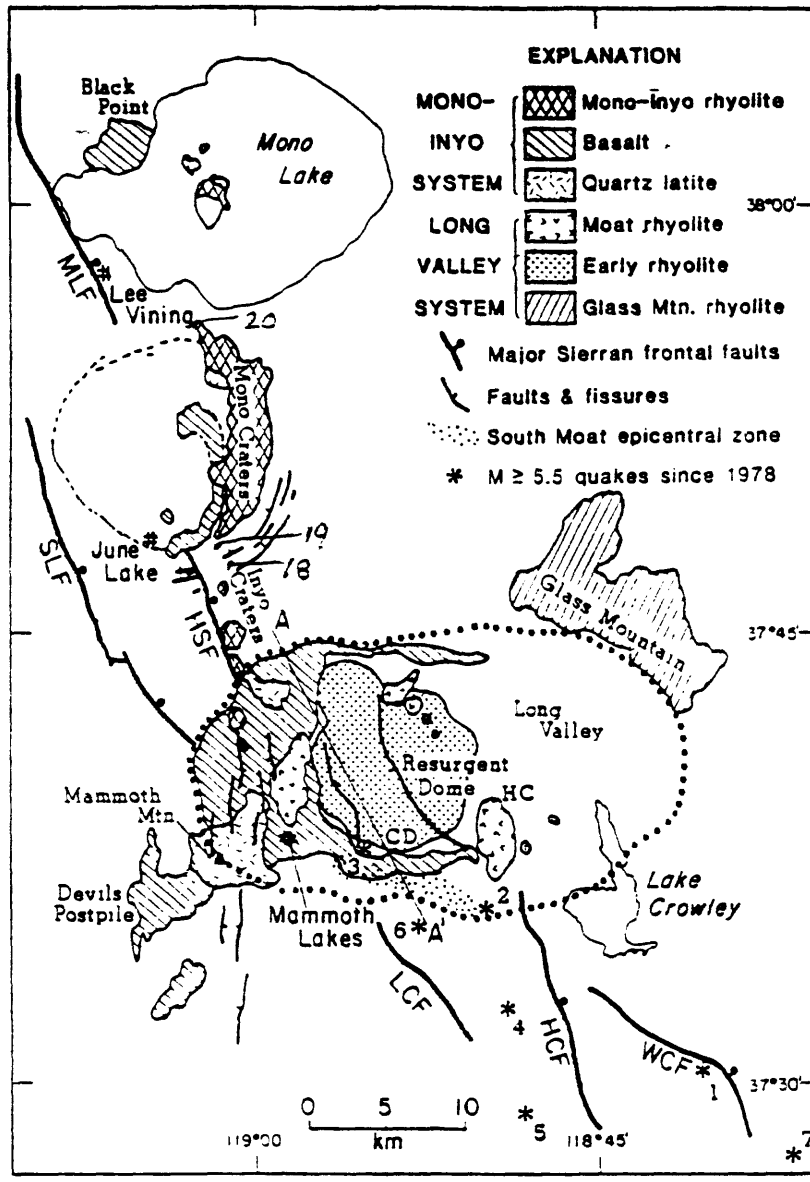

Figure 16. Geologic map of the Long Valley region showing the distribution of volcanic rocks related to Long Valley caldera magmatic system and the younger Inyo-Mono magmatic system (modified from Hill and others, 1985). Field trip stops 18, 19, and 20 are shown by numbered dots.

Saddlebag Lake, crinoid fragments and corals in an encrinal limestone were identified aspossibly Mississippian in age (Brook and others, 1979). These rocks were tightly folded in several deformations, and the dominant, older folds plunge northwest with a vertical axial surface that strikes N.20°W. (Kistler, 1966, Brook, 1977).

Resume travel on Hwy 120 to the junction with Hwy 395 near Lee Vining, CA (8.0 mi.) and turn south (right) on Hwy 395. Continue south 25.1 miles to the Mammoth Lakes turnoff, Hwy 203. Continue to the town of Mammoth Lakes (about 2.8 mi.) where we will have lodging and from which the trip will resume in the morning.

Day 4. Mammoth Lakes, Mono Craters, and Saddlebag Lake.

0.0 (0.0) Leave lodging in Mammoth Lakes on Hwy 203 and drive 2.8 miles to the Hwy 395 junction. Turn north on Hwy 395 and drive 10.2 miles to pullout at a road cut in clast-rich Bishop Tuff on the east side of the road.

13.0 (13.0) Stop #18. Deadman Summit, Clast-rich Bishop Tuff.

The exposure in the road cut is of Bishop Tuff, a large volume silicic ash flow that produced the Long Valley Caldera (Figure 16) when it was erupted. The Bishop tuff here is very lithic-rich and contains xenoliths of granitoid cobbles, basalt, and other volcanic rocks. This volcanic extrusion was the first recognized pyroclastic welded tuff in North America (Gilbert, 1938). Sanidine from a specimen of the rock was one of the first two Pleistocene volcanic rocks dated by the K-Ar technique (Evernden, Curtis, and Kistler, 1957). The age reported was about 0.83 Ma. The Bishop Tuff overlies glacial till deposited during one of the early Sierran mountain glacial epochs called the Sherwin glaciation, and its normal paleomagnetic polarity establishes a minimum age for the Brunhes-Matuyama polarity epoch boundary (Dalrymple, Cox, and Doell, 1965). Additional K-Ar dating of minerals from this rock have yielded ages that range from about 0.7 to 0.94 Ma (Evernden, Savage, Curtis, and James, 1964; Dalrymple, Cox and, Doell, 1965; Hildreth, 1977). The presently accepted age for this tuff is 0.764 ± 0.005 Ma and 0.757 ± 0.009 Ma for the lower and upper units, respectively, by $^{40}Ar/^{39}Ar$ continuous-laser fusion of sanidines (Izett and Obradovich, 1994). The range in ages by previous workers is related to incomplete gas release from sanidine during conventional K-Ar studies and xenocrystic contamination. The abundance, variety, and range in grain sizes of lithic fragments in the outcrops examined here lends credibility to the presumed role of contamination. Initial $^{87}Sr/^{86}Sr$ values of sanidine from the 722°C air-fall layer and 725°C lower unit of the tuff are around 0.7065-0.7066, whereas those from the 760°C middle unit and 790°C upper unit are around 0.7060 (Christensen and DePaolo, 1993). The temperatures are approximated from Fe-Ti oxide compositions in the tuff (Hildreth, 1977).

Proceed north from stop 18 on Hwy 395 for 3.6 miles and pull out on the broad shoulder on the right side of the highway.

16.6 (3.6) Stop #19. Vitric Bishop Tuff, South of June Lake.

This is a road cut in a much more homogeneous part of the Bishop Tuff. This view is to emphasize the variable abundance of cognate and exotic lithic fragments in the Bishop as in most other ash-flow tuffs that causes significant difficulty in extracting uncontaminated mineral separates from them for dating purposes. The tuff at this stop is strongly welded, crystal-rich, pumiceous, vitric rhyolite tuff. These exposures of Bishop Tuff are overlain by a glacial till mapped as Mono Basin till by Kistler (1966). This is clearly a pre-

Wisconsin till, younger than the Sherwin till discussed above, but its age is poorly constrained.

Continue north on Hwy 395 past the June Lake Junction (0.9 mi.) to the intersection with eastbound Hwy 120 (6.6 mi.). Turn right (east) on Hwy 120 and travel 3.0 miles to the gravel road on the left (north) to Panum Crater. Turn left on the gravel road and travel 0.9 mi. to the parking area near Panum Crater. The total distance from stop #19 is 10.5 miles.

27.1 (10.5) Stop #20. Panum Crater at the North End of the Mono Craters.

Panum Crater is the northernmost of 29 rhyolite domes and flows and one rhyodacite dome that comprise the Mono Craters (Figure 17). We will take the U.S. Forest Service trail for a brief tour of the volcanic features displayed on this dome.

Evernden, Kistler, and Curtis (1959) reported K-Ar ages of sanidine of about 6000 yr for Crater Mountain, the highest peak in the chain, and about 65,000 yr for hill 8044 at the southern end of the chain. After refinement of the analytical techniques, principally involving a HF acid leach of the sanidine to remove adsorbed atmospheric argon on crystal surfaces, the ages were redetermined at 5000 yr for Crater Mountain and to 56,000 yr for Hill 8044 (Evernden and Curtis, 1965). Subsequent dating of these volcanic edifices yielded K-Ar ages of sanidine at 11,500, 9,000, and 10,900 yrs (Dalrymple, 1968) and 5400-6700 yrs by obsidian hydration-rind dating (Wood, 1983) for Crater Mountain. Friedman (1968) estimates the age of Hill 8044 at 7,900-9,500 yrs by obsidian hydration rind-dating, whereas Dalrymple reported an age of 8,700±400 yrs for sanidine by the K-Ar technique. Hu, Smith, Evensen, and York (1993) reported ages determined by ^{40}Ar-^{39}Ar laser probe methods from 10,750±1570 yr to 14,350±2090 yr for sanidines from five of the domes that were dated at about 6000 to 12000 yrs by K-Ar techniques by Dalrymple (1968). After 35 years, the technological advances in extracting and measuring argon from minerals in young rocks indicates that in the near future a precise time span of eruption may be established for this chain of rhyolite domes and associated flows.

While we are in Mono Basin, we are well east of the Sierran front and have an excellent view of the Triassic granite of Lee Vining Canyon, which stands out as a gray band overlain by a roof pendant of red-brown Paleozoic metasedimentary rocks along the Dana Plateau. We will be examining the granite and its abundance of mafic enclaves in the next three stops. Other features include the impressive moraines of Bloody Canyon, where the major Wisconsin moraines cut across a pair of older laterals, possibly related to the older till observed overlying the Bishop Tuff at Stop 19. We should also point out Pahoa Island in Mono Lake, where a drill hole penetrated Bishop Tuff between depths of 1350 and 1625 feet. Projection of the Bishop Tuff horizon south of Panum Crater north to Pahoa Island indicates a probable normal fault displacement of 1400 to 2800 feet (Kistler, 1966b).

Leave the Panum Crater parking area by the same route we came in, return to Hwy 120 (0.9 mi.), and turn right (west). Continue west on Hwy 120 (3.0 mi.) to the junction with Hwy 395 and turn right (north). Follow Hwys 395 and 120 north (4.7 mi.) to the Hwy 120 turn off (Tioga Pass Road/Yosemite National Park) and turn left (west) up Lee Vining Canyon. This is the reverse of the route we followed from Yosemite yesterday. Proceed west up Hwy 120 toward Tioga Pass for 3.5 miles (observing mileage carefully), passing several unpaved roads on the left. Turn left off Hwy 120 and immediately right onto the Lee Vining Canyon Power Road, which becomes unpaved. Travel 0.6 miles and stop at outcrops of the granite of Lee Vining Canyon on the right (north) side of the road and pull off the road.

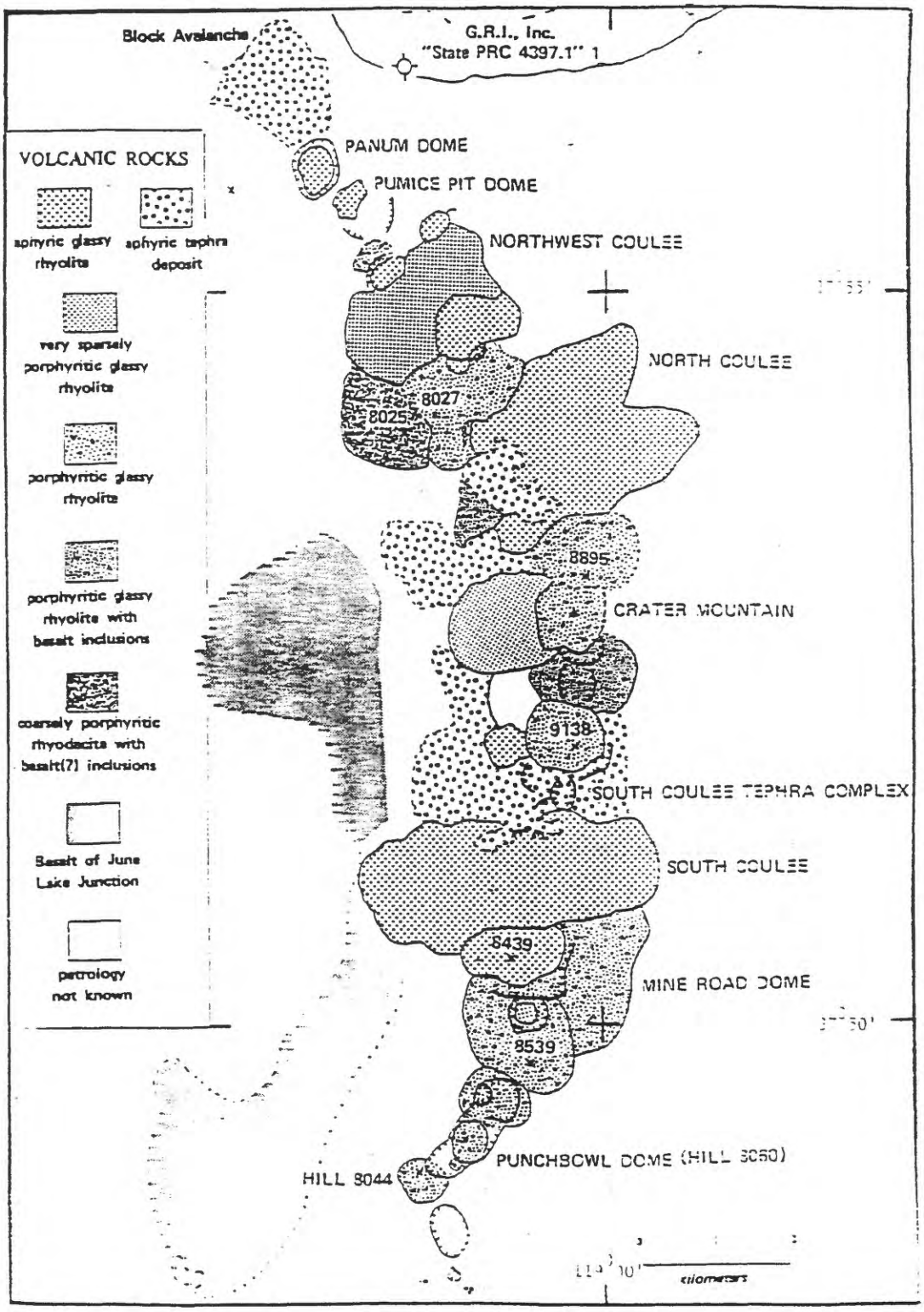

Figure 17. Geologic map of the Mono Craters and domes (modified from Wood, 1983). Field trip stop 20 is Panum Dome, the northernmost volcano in the chain.

39.8 (12.7) Stop #21. Enclave-rich Lee Vining Canyon Granite.

This is the first of three stops in the granite of Lee Vining Canyon to observe examples of the widest mafic-enclave zone reported in granitoid rocks in the Sierra Nevada. The zone generally follows the margins of the pluton and is broad enough to be shown as a pattern in the granite on the geologic map of the Mono Craters quadrangle (Kistler, 1966). Stop #21 is the first of these, located very near the granite contact with red-brown-weathering metasedimentary rocks seen above in the steep canyon wall to the north. A large block of red-brown weathering quartzite is found beside the outcrop. The low magnetic susceptibility of the enclaves and the occurrence of the enclave zone adjacent to the low-susceptibility wall rocks raises the possibility that the enclaves may have originated by stoping of the metasedimentary rock roof during emplacement. Intrusive relations between the granite and the enclaves and our chemical and isotopic measurements are not consistent with this however. We shall describe these geochemical results together, followed by more detailed discussion of the stops.

The granite of Lee Vining Canyon is one of the first Triassic granitoid rocks identified in the Sierra Nevada. A three-point Rb-Sr whole-rock isochron from specimens collected during mapping the Mono Craters quadrangle yielded 206±20 Ma with initial $^{87}Sr/^{86}Sr$ = 0.7065 (Kistler, 1966b; Evernden and Kistler, 1970). Five additional specimens were added to these for an isochron age of 212.4±8 Ma with initial $^{87}Sr/^{86}Sr = 0.70614$ (Kistler and Swanson, 1981). We have added three more specimens from the stops visited on this trip and the 11-point isochron yields an age for the granite of 216±6 Ma with initial $^{87}Sr/^{86}Sr = 0.7059\pm3$. Bulk-population U-Pb ages of zircon from specimens of the granite of Lee Vining Canyon of 203 Ma and from a cross-cutting dike of 211 Ma have been reported by Chen and Moore (1982). These were collected 10 to 12 miles south of the Lee Vining Canyon stops, near Silver Lake in the June Lake Loop.

Rb-Sr analyses of six mafic enclaves from the three Lee Vining Canyon stops *are colinear with the host granite*. This relationship relates the enclaves to the host magma rather than to incorporated wall rock, but does not completely eliminate a possible isotopic equilibration of the enclaves with the magma. Combined results of all specimens, enclaves and host granite, yield an isochron age of 216±5 with initial $^{87}Sr/^{86}Sr = 0.70579\pm3$ (Figure 18).

Magnetic susceptibility is quite variable in host granite, mafic enclaves, and a synplutonic mafic dike in the enclave zone. Figure (19) shows $\varepsilon_{Nd}(0)$ plotted against magnetic susceptibility for several enclaves, two host granites, and a synplutonic dike from the third Lee Vining Canyon stop. Each rock type has a characteristic Nd isotopic value, but no apparent correlation with susceptibility values. A similar lack of correlation exists between Rb/Sr and magnetic susceptibility in the mafic-enclave and host-granite samples. This result is somewhat surprising in view of the correlation between initial $^{87}Sr/^{86}Sr$ and magnetic susceptibility documented by Bateman, Dodge, and Kistler (1991) in the Bass Lake Tonalite east of the Coarse Gold roof pendant (Stops 5 and 6 in this field guide). Other than the obvious variability in magnetite content observed in thin-sections of both the host granite and the mafic enclaves, we can not yet offer an explanation for the wide range in susceptibility observed in this enclave-rich zone.

The exposure at stop #21 is a complex intrusive contact with a large pendant of metamorphosed sedimentary rocks. Flattened and elongated, subvertical mafic enclaves parallel foliation in the host granite and the pluton-metasedimentary rock interface. Both the granite and the mafic enclaves exhibit evidence of post-consolidation shearing, documenting substantial tectonism of the rocks after cooling. The magnetic susceptibility

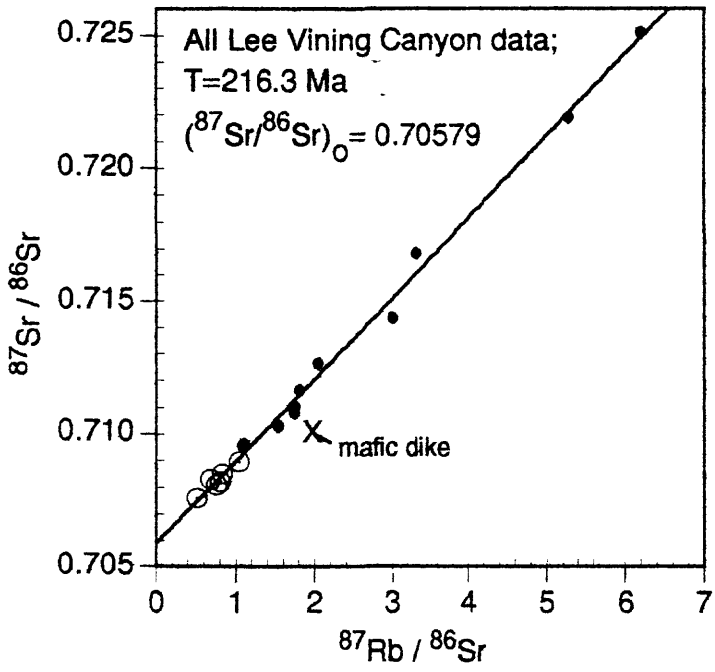

Figure 18. Rb-Sr whole-rock isochron plot for specimens of host granite (diamonds), mafic inclusions (circled dots), and a synplutonic dike of the granite of Lee Vining Canyon. Sources of data are given in the text.

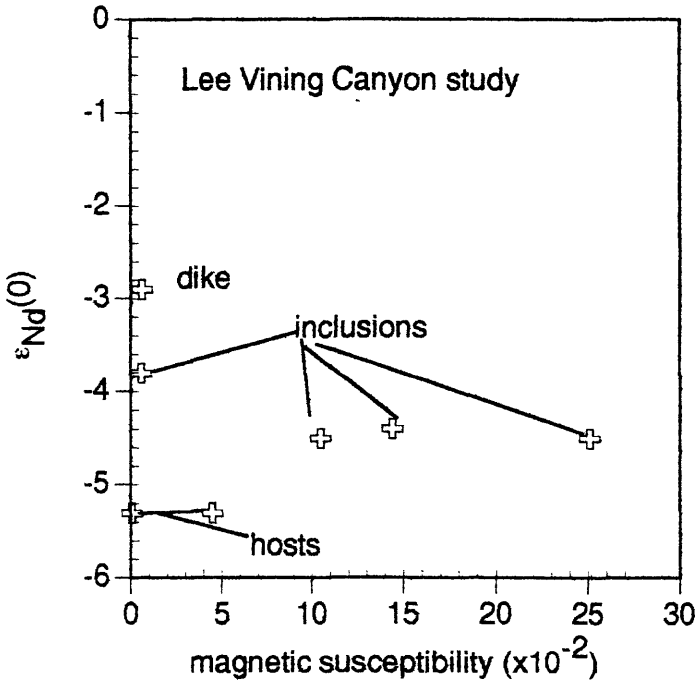

Figure 19. Plot of $\varepsilon_{Nd}(0)$ vs magnetic susceptibility in SI units for specimens of granite of Lee Vining Canyon host rocks, mafic inclusions, and a synplutonic dike.

of the granite of Lee Vining Canyon at this stop averages about 0.09 units on the Kappa meter. This low susceptibility palces the granite at this location in the ilmenuite-series. Magnetic susceptibilities this low for the granitoid rocks in this part of the Sierra Nevada are uncommon, but may be due locally to reducing conditions during interaction of the granitic magma with intruded sedimentary rocks during emplacement. The mafic enclaves have magnetic susceptibility that averages about 0.22 units on the Kappa meter.

Continue west 1.1 miles on the Lee Vining Canyon Power Road to the next exposures of the granite of Lee Vining Canyon at 7600' elevation on Lee Vining Creek.

40.9 (1.1) Stop #22. Lee Vining Canyon Granite, Second Stop.

The rock here is a biotite granite with flattened enclaves and mafic schlieren. The outcrops of granite here are farther from the contact with the metamorphosed sedimentary rocks than at Stop #21, yet contain abundant mafic enclaves. Magnetic susceptibility of the host granitic rock ranges from about 4 to 11 Kappa meter units and averages about 8 units. Measured susceptibility of mafic enclaves ranges from 0.34 to 25 units. A correlation between the susceptibilities of the enclaves and those of the host granite is apparent, with average values rising and falling together. Susceptibilitiy of the host granite adjacent to the enclaves covaries with that of the enclave, with higher susceptibilities near high susceptibility enclaves and lower values near low susceptibility ones. This local trend toward equilibration of the chemical compositions of ferromagnetic minerals demonstrates two important conclusions about enclave genesis. First, because the Rb-Sr and Sm-Nd systematics of the enclaves and the host granite are already in equilibrium, that equilibrium must have been achieved much earlier in the magmagenesis than the oxidation state of Fe. If the oxidation state of Fe and magnetic susceptibility are originally established at initial crystallization, then isotopic equilibrium must have been established in a common source region or between magmatic entities *prior* to crystallization of magnetite. Granoblastic textures within the enclaves suggest recrystallization, but acicular apatite provides evidence for quenching. Enclaves are broken and intruded by the host granite, but the granite is also cut by later mafic phases. We suggest that comagmatic relationships existed between two or more magmas. Some of the enclaves may represent early mafic segregations, possibly forming during "side-wall crystallization", that have been disrupted by subsequent flow of the granite, broken to smaller blocks, and carried along the crystallizing margin of the pluton by the magma. Others appear to be disrupted portions of mafic dikes that intruded the still flowing magma, formed blocks or pillows, and were further broken, recrystallized, and dispersed by subsequent flow within the granite. Where the chemical compositions or oxidation states of ferromagnetic minerals between the enclaves and adjacent magma were different, local interactions could cause the susceptibility of one to approach the other. The identical Sr and Nd initial ratios in the enclaves and host granite occurring between phases with different abundances of magnetite argues against a solid-liquid or solid-state equilibration of the isotopic abundances. That is, for the enclaves to represent wall-rock inclusions, the isotopic ratios of the wall rock must have been fortuitously identical to that of the granite of Lee Vining Canyon, because isotopic equilibration occurring without that of oxidation state seems improbable. Additional detailed studies of magnetic minerals, major- and minor-element chemistry, and stable isotope variations will be necessary to evaluate this argument. Any alternative origin for the enclaves, however, must be consistent with the observation of isotopic equilibrium between different enclaves, enclaves and host granite, and locally within the granite coexisting with disequilibrium in magnetic susceptibility.

Continue west on the Power road, reaching Stop #23, a dark gray to black mafic dike on the north side of the road at 0.3 miles. Parking is limited to a widening on the left and larger vehicles may need to continue to a campground or the end of the road at the Lee

Vining Canyon Powerhouse to turn around and return (1.3 miles in each direction). Upon returning, pull off on the south (right) side of the road.

41.2 (0.3) Stop #23. Lee Vining Canyon Granite, Third Stop.

Here, the granite of Lee Vining Canyon has few mafic enclaves, but includes a dark gray to black dike. The magnetic susceptibility of the dike is about 0.68±0.20, whereas that in the unaffected host granite varies from about 4.5 to 10 Kappa-meter units at a distance from the dike. Granite susceptibility decreases toward the dike and is uniformly low immediately adjacent to it, where values range from 0.6 to about 2.0 Kappa-meter units. The lowest susceptibilities in the host are at the contact with the dike. It might be suggested that a mixing of magmas has occurred between the high magnetic susceptibility (leucocratic) and low susceptibility (mafic dike) phases. Because no visible change in character or co-mingling of phases is noted, however, we find no evidence to support this. The susceptibility results probably indicate a contact metamorphism of the host granite by the mafic dike, well after cooling of the granite. This is consistent with Rb-Sr results for the mafic dike, which even considering experimental error, are not co-linear with data from the host granite and mafic enclaves (Figure 18). We believe the dike to be related to Cretaceous magmatism and is not synplutonic with the granite of Lee Vining Canyon.

Return the 2.0 miles on the Lee Vining Canyon Power Road to Hwy 120 and turn left (west) toward Tioga Pass. Drive 6.5 miles up the canyon on Hwy 120, past Ellery Lake about one-half mile to the turnoff on the north (right) side of the highway to Junction Campground and Saddlebag Lake Dam. Drive 2.5 miles up the road to the parking area at Saddlebag Lake Campground.

52.2 (11.0) Stop #24. Saddlebag Lake and Triassic Volcanic Neck.

Most of the plutons in the Sierra Nevada apparently did not vent to the surface and produce volcanic facies. However, Kistler and Swanson (1981) described and documented a small pluton in the Mono Craters quadrangle south of here as a volcanic neck and the source of 100-Ma volcanic rocks called the Minarets sequence. Here at Saddlebag Lake, we will visit exposures of the monzonite of Saddlebag Lake, one of three small plutons of altered biotite-hornblende monzonite and mafic hypabyssal andesitic intrusive rock. These rocks intrude Late Paleozoic quartzofeldspathic hornfels, calc-silicate hornfels, and carbonaceous marble that lie unconformably below the tuffaceous sandstone, siltstone, and conglomerate at the base of Triassic volcanic units of the Koip sequence (Kistler, 1966). The conglomerate and volcanic rocks are exposed at the north end of Saddlebag Lake and along the ridge to the west of us. Rb-Sr whole-rock data from 36 specimens of the lower Koip sequence volcanic rocks and 13 specimens of the biotite-hornblende monzonites and hypabyssal andesitic intrusive rock yield an age of 228.9 ±5 Ma with initial $^{87}Sr/^{86}Sr$ = 0.7053±4 (Figure 20). The monzonite intrusion at Saddlebag Lake and its effusive equivalents, the Koip sequence, were emplaced after erosion of the Late Paleozoic sedimentary rocks.

To the north near the Virginia Lakes, a rhyolitic ash-flow tuff several tens of meters above the Koip sequence basal conglomerate yields a U-Pb zircon age of 235 to 222 Ma (Schweickert and Lahren, 1987). Data for samples of volcanic rocks of the Koip sequence from that area are included in our 228.9-Ma Rb-Sr whole-rock isochron.

Drive back down the Saddlebag Lake road to a turnout at a left turn in the road 0.4 miles south of the lake.

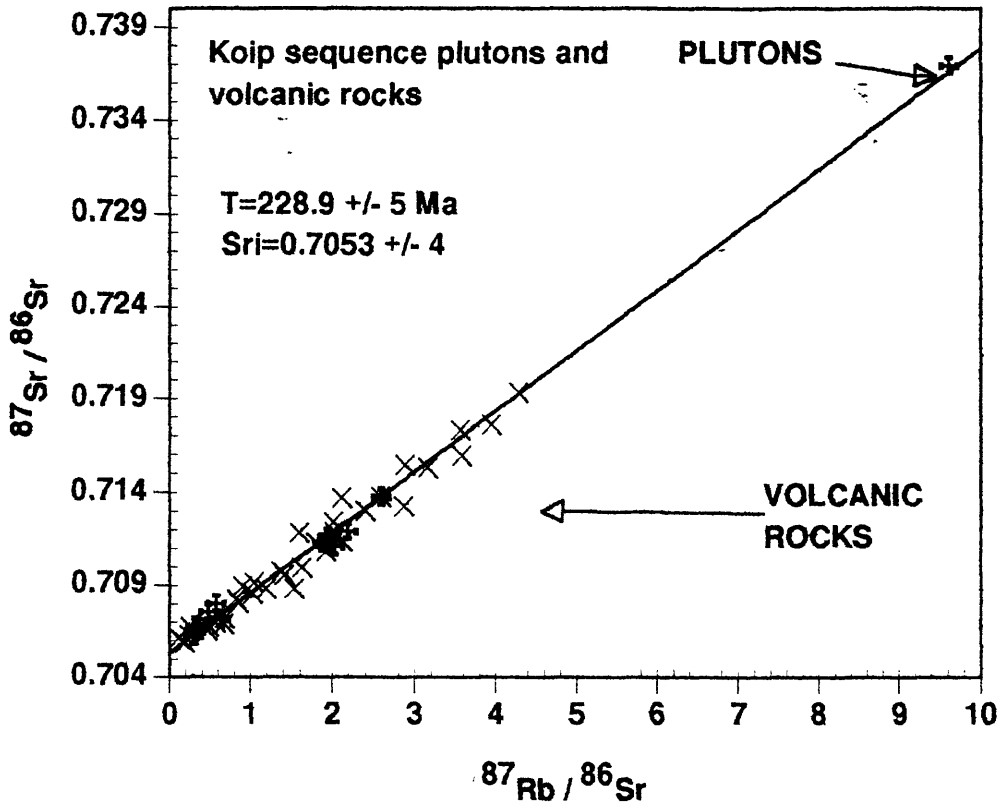

Figure 20. Rb-Sr whole-rock isochron diagram for volcanic rocks and associated plutons of the lower Koip sequence.

52.6 (0.4) Stop #25. Upper Lee Vining Canyon View Stop.

From this stop, 1300 feet south of Saddlebag Lake dam, many of the important geologic features of the crest of the Sierra Nevada and the eastern margin of the Tuolumne Intrusive Suite may be placed in perspective. Our viewpoint is on NNW-striking, nearly vertically-dipping, undifferentiated Late Paleozoic metasedimentary rocks of the unit surrounding Saddlebag Lake. Looking to the west, the contact between these strata and the overlying Triassic strata of the Koip sequence occur near the confluence of the two forks of Lee Vining Creek below us. About 1 km farther west, Jurassic volcanic strata of the upper part of the Koip sequence overlie the Triassic units. Rhyolite tuff within this part of the Koip sequence yield an Rb-Sr whole-rock isochron age of 185 Ma. Immediately west of these exposures and occupying the ridge on the horizon the Tuolumne Intrusive Suite intrudes these and older strata. Much of the ridge due west of us is Cathedral Peak Granodiorite. To the west-southwest we view White Mountain and the ridge to the south that is comprised of Half Dome Granodiorite and granodiorite of Kuna Crest.

Turning to the south, the prominent, pyramidal mountain peak in the near distance is 13,057-feet-high Mount Dana. The rocks exposed on this peak are the Early Cretaceous Dana sequence that occurs in a down-dropped block that extends from Mount Dana northwest across Tioga Pass to Gaylor Peak (Kistler, 1966). Rocks of the Dana sequence consist of interbedded metavolcanic tuffs, lapilli tuff, and flows, and metasedimentary shale, calc-silicate hornfels, and marble (Kistler, 1966; Russell, 1976) and are commonly in fault contact with the older, Koip sequence. Dips in the Dana sequence are mostly gentle, and the strata are folded into an open, northwest-trending anticline and companion syncline with subhorizontal fold axes. Fold axes in the Koip sequence vary with location and commonly have steeper plunges, but define a plane that coincides with the orientation of the axial surface of the folds in the Dana sequence. This structural geometry indicates that an older generation of folds in the Koip sequence with more northerly-trending axial surfaces formed prior to the deposition of the overlying and unconformable Dana sequence (Kistler, 1966; Russell, 1976). Kistler and Swanson (1981) reported a Rb-Sr whole-rock age of 118±11 Ma with initial $^{87}Sr/^{86}Sr = 0.70578$ for three specimens of a tuffaceous rock collected from the upper part of the Dana sequence approximately 60 ft. below the summit of Mount Dana. Four additional whole-rock specimens that include andesite, basalt, and porphyritic latite from exposures near the base of the sequence just to the north of Tioga Pass, and a rhyodacite tuff, probably the oldest exposed unit in the sequence, from the southwest flank of Mount Dana yield a Rb-Sr whole-rock isochron age of 120.3±9 Ma with initial $^{87}Sr/^{86}Sr = 0.70482$ (Figure 21).

Light-colored rock east of Mount Dana is the granite of Ellery Lake, whereas the layered, brown-weathering rocks are the Late Paleozoic metamorphosed sedimentary rocks, continuous with those intruded by the monzonite of Saddlebag Lake and on which we stand.

Continue south about 2.1 miles down to Hwy 120. Turn left (east) and descend Lee Vining Canyon on Hwy 120 to Hwy 395. At the junction with Hwy 395 turn right (south) and drive 25.1 miles to the Mammoth Lakes turnoff. Turn right and return to Mammoth Lakes (2.8 miles).

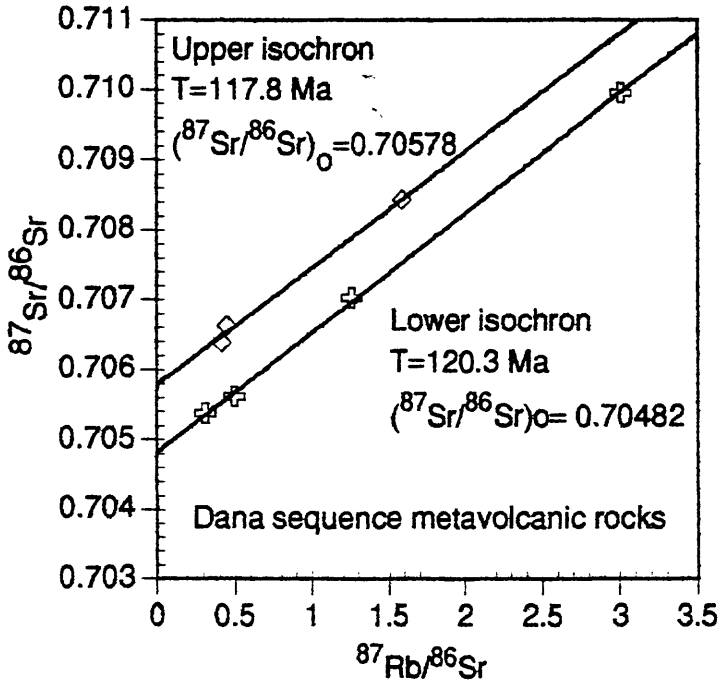

Figure 21. Rb-Sr whole-rock strontium evolution isochron plot for volcanic rocks and associated hypabyssal plutons of the Dana sequence.

Day 5. Mammoth Lakes to Berkeley, CA.

The trip back to Berkeley will follow many of the same roads traveled the last two days through Yosemite National Park. Leave Mammoth Lakes on Hwy 203 and drive 2.8 miles to the Hwy 395 junction. Turn north on Hwy 395 and continue 25.1 miles to the junction with westbound Hwy 120. Turn left (west) on Hwy 120 and proceed across Yosemite National Park 58.8 miles to Crane Flat and the intersection with the Big Oak Flat Road. Turn right at the intersection with Hwy 120, as it follows the Big Oak Flat Road to the west. We will follow Hwy 120 west, leaving through the west entrance of Yosemite National Park, and passing through Buck Meadows (20.8 miles) and Groveland (another 10.5 miles) to the top of Priest Grade (3.4 miles west of Groveland), a steep, slow decline of 4.6 miles to Moccasin at the intersection with Hwy 49. Continue west 36.5 miles on Hwy 120 to the city limits of Oakdale, CA. We will stretch, use restroom facilities at a local hamburger restaurant, and have lunch on the bus or participants may choose to buy hamburgers. We will proceed west through Oakdale, making a right turn in the center of town to stay on Hwy 120. We pass through Escalon, with its left turn to stay on Hwy 120, and continue to the junction with Hwy 99. We turn south with Hwy 120 on Hwy 99 for 1 mile to the Hwy 120 (west) exit. Leaving Hwy 99, we follow Hwy 120 to its junction with Interstate Highway 5 (south). Continue south on I-5 to the next exit, I-205 (west). We take I-205 west to its junction with I-580 and continue west on I-580 back to Berkeley.

References Cited

Ague, J.J., and Brimhall, G.H., 1988, Magmatic arc asymmetry and distribution of anomalous plutonic belts in the batholiths of California: Effects of assimilation, crustal thickness, and depth of crystallization: Geological Society of America Bulletin, v. 100, p.912-927.

Barbarin, Bernard, Dodge, F.C.W., Kistler, R.W., and Bateman, P.C., 1989, Mafic inclusions, aggregates, and dikes in granitoid rocks, central Sierra Nevada batholith, California---Analytic data: U.S. Geological Survey Bulletin 1899, 28 p.

Bateman, P.C., 1992, Plutonism in the central part of the Sierra Nevada batholith: U.S. Geological Survey Professional Paper 1483, 186 p.

Bateman, P.C., and Chappell, B.W., 1979, Crystallization, fractionation, and solidification of the Tuolumne Intrusive Series, Yosemite National Park, California: Geological Society of America Bulletin, pt.1, v. 90, p.465-482.

Bateman, P.C., Dodge, F.C.W., and Kistler, R.W., 1991, Magnetic susceptibility, and relation to initial 87Sr/86Sr for granitoids of the central Sierra Nevada, California: Journal of Geophysical Research, V. 96, no. B12, p. 19,555-19,568

Bateman, P.C., Kistler, R.W., and DeGraff, J.V., 1984, Courtright intrusive zone, Sierra National Forest, Fresno County, California: California Geology, v. 37, no. 5, p. 91-98

Brook, C.A., 1977, Stratigraphy and structure of the Saddlebag Lake roof pendant, Sierra Nevada, California: Geological Society of America Bulletin, v. 88, p. 321-334.

Brook, C.A., MacKenzie, Gordon, Jr., Mackey, M.J., and Chetlat, G.F., 1979, Fossiliferous upper, Paleozoic rocks and their structural setting in the Ritter Range and Saddlebag Lake roof pendants, central Sierra Nevada, California: Geological Society of America Abstracts with Programs, v.11, p. 70.

Calkins, F.C., 1930, The granitic rocks of the Yosemite region, Appendix of Matthes, F.E., Geologic history of the Yosemite Valley: U.S. Geological Survey Professional Paper 160, p. 120-129

Chen, J.H., and Moore, J.G., 1982, Uranium-Lead isotopic ages from the Sierra Nevada batholith, California: Journal of Geophysical Research, v. 87, no. B6, p. 4761-4784.

Chen, J.H., and Tilton, 1991, Applications of lead and strontium isotopic relationships to the petrogenesis of granitoid rocks, central Sierra Nevada, California: Geological Society of America Bulletin, v. 103, no. 4, p. 439-447.

Christensen, J.N., and DePaolo, 1993, Time scales of large volume silicic magma systems: Sr isotopic systematics of phenocrysts and glass from the Bishop tuff, Long Valley California: Contributions to Mineralogy and Petrology, v. 113, p. 100-114.

Curtis, G.E., Evernden, J.F., and Lipson, J., 1958, Age determinations of some granitic rocks in California by the potassium-argon method: California Division of Mines Special Report 54, 16 p.

Dalrymple, G.B., 1968, Potassium-argon ages of recent rhyolites of the Mono and Inyo Craters, California: Earth and Planetary Science Letters, v. 3, no. 4, p. 289-298.

Dalrymple, G.B., Cox, A., and Doell, R.R., 1965, Potassium-argon age and paleomagnetism of the Bishop Tuff, California: Geological Society of America Bulletin, v. 76, p. 665-674.

DePaolo, D.J., 1981, A neodymium and strontium isotopic study of the Mesozoic calc-alkaline granitic batholiths of the Sierra Nevada and Peninsular Ranges, California, in Granites and Rhyolites: Journal of Geophysical Research, Series B, v. 86, no. 11, p. 10470-10488.

Dodge, F.C.W., and Calk, L.C., 1986, Lake Eleanor quadrangle, central Sierra Nevada, California--Analytical data: U.S. Geological Survey Bulletin 1585, 20 p.

Dodge, F.C.W., and Calk, L.C., 1987, Geologic map of the Lake Eleanor quadrangle, central Sierra Nevada, California: U.S. Geological Survey Geologic Quadrangle Map GQ 1639, scale 1:62,500.

Dodge, F.C.W., and Kistler, R.W., 1990, Some additional observations on inclusions in the granitic rocks of the Sierra Nevada: Journal of Geophysical Research, v.95, no.B11, p. 17841-17848

Evernden, J.F., and Curtis, G.H., 1965, The potassium-argon dating of Late Cenozoic rocks in East Africa and Italy: Current Anthropology, v. 6, no. 4, p. 343-385.

Evernden, J.F., Curtis, G.H., and Kistler, R.W., 1957, Potassium-argon dating of Pleistocene volcanics: Quaternaria, v. 4, p. 13-17.

Evernden, J.F., and Kistler, R.W., 1970, Chronology of emplacement of Mesozoic batholithic complexes in California and western Nevada: U.S. Geological Survey Professional Paper 623, 42 p.

Evernden, J.F., Kistler, R.W., and Curtis, G.H., 1959, Cenozoic time scale of the west coast: Geological Society of America Program with Abstracts, Cordilleran Section, Tucson, Arizona, p. 24.

Evernden, J.F., Savage, D.E., Curtis, G.H., and James, G.T., 1964, Potassium-argon dates and the Cenozoic mammalian chronology of North America: American Journal of Science, v. 262, p. 145-198.

Fleck, R.J., and Kistler, R.W., 1994, Chronology of multiple intrusion in the Tuolumne Intrusive Suite, Yosemite National Park, Sierra Nevada, California: U.S. Geological Survey Open-File Report, in press.

Friedman, I., 1968, Hydration rind dates rhyolite flows: Science, v.159, p. 878-881.

Gilbert, C.M., 1938, Welded tuff in eastern California: Geological Society of America Bulletin, v. 49, p.1829-1862.

Hildreth, E.W., 1979, The Bishop tuff: evidence for the origin of compositional zonation in silicic magma chambers: Geological Society of America Special Paper 180, p. 43-75.

Hill, D.P., Bailey, R.A., and Ryall, A.S., 1985, Active tectonic and magmatic processes beneath Long Valley caldera, eastern California: an overview: Jour. Geophys. Res., v.90, no.B13, p. 11,111-11,120.

Hu, O., Smith, P.E., Evensen, N.M., and York, D., 1993, Extending the ^{40}Ar-^{39}Ar laser probe method into the Carbon-14 age range: single crystal dating of sanidines from Mono Crater, California: EOS, Transactions, American Geophysical Union, v. 74, no. 16, p. 339.

Ishihara, Shunso, 1977, The magnetite-series and ilmenite-series granitic rocks: Mining Geology, v. 27, p. 293-305

Izett, G.A., and Obradovich, J.D., 1994, $^{40}Ar/^{39}Ar$ age constraints for the Jaramillo Normal Subchron and the Matuyama-Brunhes geomagnetic boundary: Journal of Geophysical Research, v. 99, no. B2, p.2925-2934.

Kistler, R.W., 1966a, Geologic map of the Mono Craters Quadrangle, Mono and Tuolumne Counties, California: U.S. Geological Survey Geologic Quadrangle Map GQ-462, scale 1:62,500.
Kistler, R.W., 1966b, Structure and metamorphism in the Mono Craters quadrangle, Sierra Nevada, California: U.S. Geological Survey Bulletin 1221-E, 53 p.
Kistler, R.W., 1973, Geologic Map of the Hetch Hetchy Reservoir quadrangle, Yosemite National Park, California: U.S. Geological Survey Geologic Quadrangle Map GQ 1112, scale 1:62,500.
Kistler, R.W., 1990, Two different lithosphere types in the Sierra Nevada: In Anderson, J.L., ed., The Nature and Origin of Cordilleran Magmatism, Geological Society of America Memoir 174, p. 221-281
Kistler, R.W., 1993, Mesozoic intrabatholithic faulting, Sierra Nevada, California: In Dunne, G., and McDougall, K., eds., Mesozoic Paleogeography of the western United States-II, Pacific Section SEPM, Book 71, p. 247-262
Kistler, R.W., Bateman, P. C., and Brannock, W.W., 1965, Isotopic ages of minerals from granitic rocks of the central Sierra Nevada and Inyo Mountains, California: Geological Society of America Bulletin, v.76, no.2, p.155-164.
Kistler, R.W., Chappell, B.W., Peck, D.L., and Bateman, P.C., 1986, Isotopic variations in the Tuolumne Intrusive Suite, central Sierra Nevada, California: Contributions to Mineralogy and Petrology, v.94, p.205-220.
Kistler, R.W., and Dodge. F.C.W., 1966, Potassium-argon ages of coexisting minerals from pyroxene-bearing granitic rocks in the Sierra Nevada, California: Journal of Geophysical Research, v.71, No. 8, p.2157-2161.
Kistler, R.W., and Peterman, Z.E., 1973, Variations in Sr, Rb, K, Na, and initial 87Sr/86Sr in Mesozoic granitic rocks and intruded wall rocks in central California: Geological Society of America Bulletin, v.84, p.3489-3512.
Kistler, R.W., and Swanson, S.E., 1981, Petrology and geochronology of metamorphosed volcanic rocks and a middle Cretaceous volcanic neck in the east-central Sierra Nevada, California: Journal of Geophysical Research, v.86, no. B11, p. 10,489-10,501.
Mack, S., Saleeby, J.B., Ferrell, J.E., 1979, Origin and emplacement of the Academy pluton, Fresno County, California: Summary: Geological Society of America Bulletin, Part 1, v. 90, p.321-323
Naeser, C.W. and Dodge, F.C.W., 1969, Fission-track ages of accessory minerals from granitic rocks of the central Sierra Nevada batholith, California: Geol. Soc. America Bull., v.80, p. 2201-2212.
Russell, S.J., 1976, Geology of the Mount Dana roof pendant, central Sierra Nevada, California [M.A. thesis]: Fresno, California State University, 71 p.
Saleeby, J., Sharp, W., 1980, Chronology of the structural and petrologic development of the southwest Sierra Nevada foothills, California: Geological Society of America Bulletin, Part II, p. 1416-1535.
Schweickert, R.A., and Lahren, M.M., 1987, Continuation of Antler and Sonoma orogenic belts to the eastern Sierra Nevada, California, and Late Triassic thrusting in a compressional arc: Geology, v. 15, p. 270-273.
Shaw, H.F., Chen, J.H., Saleeby, J.B., and Wasserburg, G.J., 1987, Nd-Sr-Pb systematics and age of the Kings River ophiolite, California: implications for depleted mantle evolution: Contributions to Mineralogy and Petrology, v. 96, p.282-290
Stern, T.W., Bateman, P.C., Morgan, B.A., Newell, M.F., and Peck, D.L., 1981, Isotopic U-Pb ages of zircon from the granitoids of the central Sierra Nevada: U.S. Geological Survey Professional Paper 1185, 17p.
Tobisch, O.T., Renne, P.R., and Saleeby, J.B., 1993, Deformation resulting from regional extension during pluton ascent and emplacement, central Sierra Nevada, California: Journal of Structural Geology, v. 15, no 3-5, p 609-628

Wood, S.H., 1983, Chronology of Late Pleistocene and Holocene volcanics, Long Valley and Mono Basin Geothermal Areas, eastern California: U.S. Geological Survey Open File Report 83-747, 76p.